TYPE Original Research
PUBLISHED 19 November 2025
DOI 10.3389/feart.2025.1710366



OPEN ACCESS

EDITED BY
Jianhua He,
Chengdu University of Technology, China

REVIEWED BY
Junjun Shen,
Yangtze University, China
Chuan Xu,
Chengdu University of Technology, China

*CORRESPONDENCE Hongxiang Jin, ■ 19182163086@163.com

RECEIVED 22 September 2025 REVISED 25 October 2025 ACCEPTED 31 October 2025 PUBLISHED 19 November 2025

CITATION

Jin H (2025) Hydrocarbon charging processes of deep fractured-vuggy dolomite reservoirs in the Ediacaran Dengying Formation, Southern Sichuan Basin, SW China. *Front. Earth Sci.* 13:1710366. doi: 10.3389/feart.2025.1710366

COPYRIGHT

© 2025 Jin. This is an open-access article distributed under the terms of the Creative Commons Attribution License (CC BY). The use, distribution or reproduction in other forums is permitted, provided the original author(s) and the copyright owner(s) are credited and that the original publication in this journal is cited, in accordance with accepted academic practice. No use, distribution or reproduction is permitted which does not comply with these terms.

Hydrocarbon charging processes of deep fractured-vuggy dolomite reservoirs in the Ediacaran Dengying Formation, Southern Sichuan Basin, SW China

Hongxiang Jin*

Geology Exploration and Development Research Institute, CNPC Chuanqing Drilling Engineering Co., Chengdu, China

The largest carbonate gas field in China has been discovered in the Cambrian-Ediacaran of Central Sichuan Basin. Despite the enormous resource potential, differences in hydrocarbon-charging conditions have limited subsequent exploration and development in Southern Sichuan Basin. Based on biomarker compounds, hydrocarbon generation history, homogenization temperature of fluid-inclusions, carbon isotopes and other data, the key scientific issues faced in the restoration of hydrocarbon-charging processes were analyzed, and the evolution models of Ediacaran petroleum system in different areas were established. The results show that: (1) The quality of the Cambrian Maidiping source rocks is better than the Qiongzhusi Formation, and its kerogen type is Type I. The maturity of the Maidiping source rocks is high and in the stage of over-matured evolution. (2) Dengying natural gas is a mixed product of oilcracking gas and kerogen-cracking gas, and the sources and origin vary greatly in different areas and wells. Natural gas in the WY Gas Field comes from the Qiongzhusi source rocks, while the proportion of Maidingdi source rocks for gas supply in the fourth Member of the AY Gas Field and second Member of the Ziyang area is significantly higher. As the main source rock, the Qiongzhusi Formation entered the hydrocarbon-generation process from the late Silurian and began to uplift and end hydrocarbon-generation in the late Cretaceous. The Permian and Triassic are the main oil-generation periods. The gas-generation period lasted from the Late Permian to the end of the Early Cretaceous, with the Jurassic being its main gas-generation period. The hydrocarbon-charging processes of the Ediacaran petroleum system in Southern Sichuan went through three stages: the formation stage of paleo-oil reservoirs in the Caledonian-Hercynian period, the cracking stage of oil into gas in the Indosinian-Yanshanian period, and the adjustment and finalization stage of gas reservoirs in the Himalayan period.

KEYWORDS

Ediacaran petroleum system, deep fractured-vuggy dolomite, hydrocarbon charging, source rock, Southern Sichuan Basin

1 Introduction

The majority of oil and gas production worldwide comes from shallow and medium-depth hydrocarbon reservoirs (Al-Shami et al., 2023; Prather et al., 2023; Hattori and Radjef, 2024). With advancements in industrial technology and the need for sustained production (Hagstrom et al., 2024; Larue et al., 2024), reservoirs buried deeper than 4,000 m are increasingly becoming key targets for hydrocarbon exploration (Gu et al., 2023). Deep sandstone and dolomite reservoirs, even shale reservoir, can maintain significant porosity under favorable burial and diagenetic conditions (Worden et al., 2020; Wang et al., 2025; Yang et al., 2025). Remarkably, reservoirs can still produce commercially viable oil and gas flows even when buried beyond 6,000 m (Ye et al., 2024). In the presence of deep reservoirs, determining the quality and distribution of source rocks, along with the factors that influence hydrocarbon accumulation, is essential for reducing exploration risks in these areas.

The oil and gas exploration of the Caledonian paleo-uplift in the Sichuan Basin began in the mid-1950s. During this period, the WY Gas Field was discovered. However, due to a lack of detailed studies on source rocks and hydrocarbon accumulation, the AY Gas Field was not identified until 2011 (Ma et al., 2019; Fang et al., 2024). In May 2020, the Well PT-1 in the north slope of Caledonian paleo-uplift obtained $121.98 \times 10^4 \,\mathrm{m}^3/\mathrm{d}$ of natural gas in the Dengying Formation second Member (Sun et al., 2017; Yang et al., 2020), demonstrating good exploration and development results. Previous studies suggest that the distribution of source rocks and the contact relationships of deep dolomite reservoirs are key factors contributing to the differences in paleo-oil sources across areas (Fang et al., 2024). The solid bitumen of the Dengying Formation in AY Gas Field mainly originates from the Lower Cambrian Maidiping Formation. The bitumen collected in north of the paleouplift primarily originates from the Lower Cambrian Qiongzhusi Formation, while the bitumen in the northern Sichuan Basin is thought to derive from the Ediacaran Doushantuo Formation (Fang et al., 2024). In the western Sichuan Basin, the natural gas in the Dengying Formation is sourced not only from the Qiongzhusi Formation but also from the Dengying third Member and the Doushantuo Formation (Luo et al., 2024). The natural gas in the Dengying Formation of the WY Gas Field primarily originates from the Qiongzhusi Formation. The gas pools in the AY Gas Field and to the north display a dual-source characteristic, deriving hydrocarbons from both the Qiongzhusi Formation and the Dengying third Member (Song et al., 2025).

Risk exploration wells such as Well JT-1 also achieved high production breakthroughs, indicating that intracratonic sag and its margins are the successor areas for further exploration of deep fractured-vuggy dolomite gas fields. At present, industrial gas flow has also been obtained in the Dengying second Member of Well HS-1 and Dengying fourth Member of Well HS-2, proving that the deep fractured-vuggy dolomite in the Southern Sichuan Basin has broad prospects for oil and gas exploration (Wei et al., 2022). Recent studies indicate that tectonic differentiation within cratonic basins plays a critical role in the formation of large oil and gas fields (Wang et al., 2024). During the Late Ediacaran, the Yangtze Block underwent extensional rifting accompanied by repeated transgression–regression cycles, forming a differentiated

platform–shelf system with multiple intracontinental rifts along its northern margin (Li et al., 2018). Thick reef–shoal deposits accumulated along platform margins, while rift troughs controlled the development of high-quality Cambrian source rocks, and early Cambrian transgression further deposited exceptionally thick black shales (200–450 m) in the craton interior (Guo et al., 2024). In the Dengying Formation, the coexistence of high-quality source rocks, large platform-margin reservoirs, long-term inherited paleouplifts and slope structures, *in-situ* accumulation of oil-cracking gas, and favorable preservation conditions collectively controlled the formation of giant gas fields (Yang et al., 2016; Fan et al., 2022).

The evolution of the rimmed shelf platform governed the development of large-scale high-quality reservoirs in the Dengying Formation, where high-energy mound-shoal deposits, modified by syndiagenetic-stage dolomitization and dissolution under the combined influence of lithofacies and karst processes, are characterized by abundant dissolution pores and fractures, considerable effective thickness, and excellent reservoir properties (Gu et al., 2019; Gu et al., 2023). Although early studies suggested that platform-margin gas reservoirs were sourced from the Lower Cambrian Qiongzhusi Formation, significant differences in gas sources between the Ediacaran Dengying Formation at platform margins and the Cambrian Longwangmiao Formation in the platform interior indicate the development of deep-water Dengying shales within rift troughs (Li et al., 2023). Multiple hydrocarbon-generation phases from the Cambrian Qiongzhusi Formation led to Early Cambrian-Middle Ordovician and Early Permian-Triassic charging events in the Dengying Formation, followed by Jurassic-Cretaceous in-situ oil-to-gas cracking. Since the Late Triassic, deeply buried foreland reservoirs gradually converted to gas, with Late Yanshanian-Himalayan tectonics further modifying their distribution (Guo et al., 2024; Shi et al., 2024; Deng et al., 2025). Two types of enrichment zones have been proposed in the Dengying Formation: a composite accumulation belt adjacent to rifts at platform margins, and a composite belt where faults overlap with grain shoals (Wang et al., 2024). Forward modeling of hydrocarbon systems further suggests that the most favorable enrichment areas in the Southern Sichuan Basin region are those combining lateral-adjacent reservoirs, over-pressure conditions, and structural trap superposition (Deng et al., 2023).

Recent sedimentary facies studies indicate that the intracratonic sag did not extend toward the southern end of the basin (Hou et al., 2021; Li et al., 2023). Under these conditions, favorable exploration targets in the southern Sichuan Basin within the Dengying Formation include intracratonic sag mounds and intra-platform mound-shoal complexes (Zeng et al., 2023). The southern Sichuan Basin, located within the Cambrian hydrocarbon generation center, provides favorable conditions for source rock development. However, the contribution of the Cambrian Maidiping Formation source rock to Dengying Formation remains uncertain. Multiple tectonic events have led to well-developed faults, making natural gas adjustment complex (Tian et al., 2023). The origin of natural gas in the Dengying Formation has long been debated (Wei et al., 2015; Su et al., 2022; Wang et al., 2023; Guo et al., 2024), and the influence of contact relationships on hydrocarbon migration and accumulation remains unclear (Shuai et al., 2023).

In this study, the Maidiping and Qiongzhusi Formation source rocks were systematically evaluated considering their high

thermal maturity. Using optimized carbon isotope comparison parameters, the genetic types of natural gas across different areas of the basin were determined. Combined with biomarker analyses, the oil and gas sources were comprehensively assessed, and the primary source rocks of each stratum were identified. Based on structural and sedimentary evolution, the hydrocarbon charging process was reconstructed, and an oil and gas accumulation model was established. This integrated evaluation of source–storage configuration in the Dengying Formation provides a solid geological basis for expanding exploration targets and offers new insights for future hydrocarbon exploration.

2 Geological setting

The study area is located in the Southern Sichuan Basin, including areas such as Weiyuan, Luzhou, and Yongchuan, with an area of approximately 25,000 km². The structural location of the study area belongs to the South Sichuan low steep fold belt and southern part of Central Sichuan gentle fold belt (Figure 1A). Due to the evolution of structural conditions and sedimentary environments, strata such as the Ediacaran Doushantuo Formation and Dengying Formation, Cambrian Maidiping Formation, Qiongzhusi Formation, Canglangpu Formation and Longwangmiao Formation have developed from bottom to top in the study area (Figure 1B). According to microbial content and sedimentary structure, the Ediacaran Dengying Formation can be divided into four members (Xu et al., 2016). Among them, the second (Z_2dn^2) and fourth Member (Z₂dn⁴) comprise microbial dolostromatolite and dololaminite. The first Member (Z_2dn^1) is mainly dolomite, and the third Member (Z₂dn³) comprises shale mudtone, and siltstone. Due to the uplift movement during the Tongwan period of the Late Ediacaran, the upper part of the second (Z_2dn^2) and fourth Member (Z2dn4) underwent erosion and extensive karstification, forming an unconformity surface (Figure 1B). The microbial mounds and mound-shoal complexes in the second and fourth Member are effective exploration targets (Ye et al., 2024).

Previous studies have identified four sets of potential source rocks in the study areas, that is the Doushantuo (Z_1 ds), Dengying third Member (Z_2 dn³), Maidiping, and Qiongzhusi formations (Li et al., 2023; Wang et al., 2025). In the Sichuan Basin, these source rocks were primarily concentrated in the intracratonic sag (Song et al., 2025). The thickest areas (>30 m) of the Doushantuo source rocks are located in the northern Sichuan Basin (Fang et al., 2024). In the intracratonic sag, the Dengying third Member mudstone has a thickness of 10–30 m (Zhao et al., 2021). The Maidiping mudstone has a thickness of 80–120 m in the intracratonic sag. The Qiongzhusi organic-rich shale/mudstone has a thickness more than 700 m (Yong et al., 2024).

3 Samples and methods

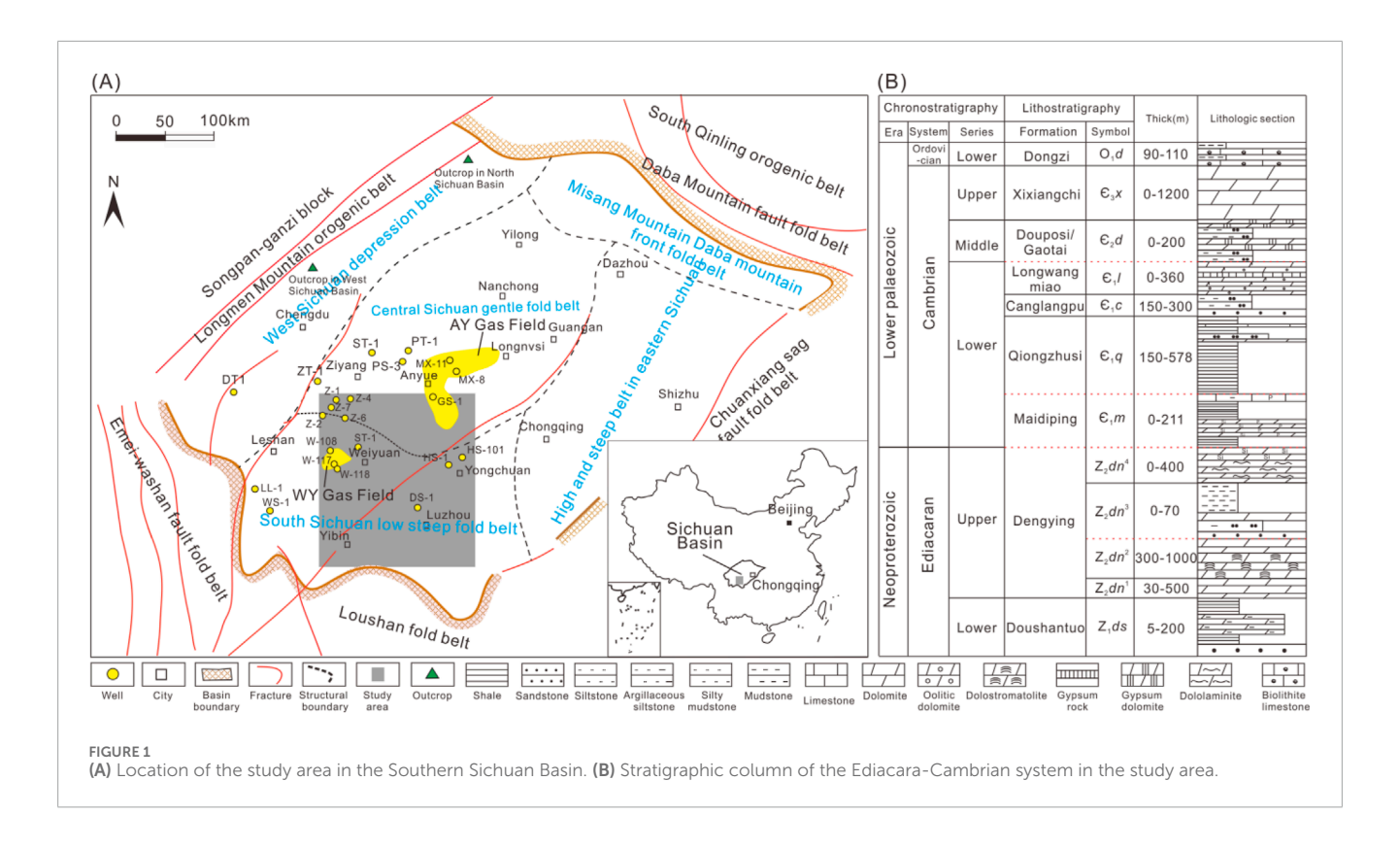
Forty samples were collected from two outcrops in Western and Northern Sichuan Basin. Sixty-six core samples and over

two hundred drilling cut samples were collected from ten drilling wells including Well Z-4, Z-1, HS-1, etc. Fifty-two drilling cut samples were used to determine total organic carbon (TOC) values. A total of forty dolomite samples were selected to determine the homogenization temperature (Th). A total of two hundred fluid-inclusions were measured for Th values. Thirty core samples were used to determine stable carbon isotopes. Nineteen solid asphalt and source rock debris samples were used to obtain chromatography-mass spectrometry.

TOC values were obtained through CS-230 Carbon and Sulfur Analyzer in State Key Laboratory of Southwest Petroleum University. Samples are placed in a ceramic crucible and subjected to combustion through high-frequency induction heating with an oxygen flow. The carbon and sulfur in the samples are oxidized, producing $\rm CO_2$ and $\rm SO_2$. These gases are then carried by the oxygen to the detection unit, where they absorb infrared energy. This absorption leads to a decrease in the energy received by the detection unit. By analyzing the reduction in infrared energy and its relationship with the concentration of the gases, we can determine the concentrations of $\rm CO_2$ and $\rm SO_2$, allowing us to calculate the amounts of carbon and sulfur in the samples.

The separation of three kerogen samples was completed at the Keyuan Engineering Technology Testing Center. The identification and maturity determination of kerogen were carried out using a vitrinite reflectance analyzer and a Zeiss Scope A1 polarizing microscope. Stable carbon isotope values were obtained through Delta Plus V Stable Isotope Mass Spectrometer in Sinopec Wuxi research institute. Bound regular steranes in the hydropyrolysates of solid bitumen and potential source rocks were obtained through Agilent 7890N gas chromatograph and LECO Pegasus-4D TOF-MS mass detector in China University of Geosciences (Beijing). The experimental process can be divided into three stages: (1) Gas Chromatography Separation: After vaporization, the sample is carried into the chromatography column by a carrier gas. Physical separation occurs based on differences in the distribution coefficients of compounds between the stationary and mobile phases. (2) Mass Spectrometry Ionization and Detection: The separated components are transferred through a heated transfer line to the ion source of the mass spectrometer (e.g., electron impact source, EI), where they are ionized in a vacuum environment to form charged ions. These ions are then separated by mass-to-charge ratio (m/z) using a mass analyzer (such as a quadrupole or time-of-flight analyzer). (3) Data Collection and Analysis: The detector records the ion intensity at different m/z values, generating mass spectra (which reflect the characteristics of compound fragments) and total ion chromatograms (TIC, which indicate the retention times and peak areas of each component).

Fluid-inclusion observation and microthermometry were performed using an Olympus BX51 microscope equipped with a ROLERA-XR infrared camera and a Linkam THMSG600 heating–freezing stage. $T_{\rm h}$ and final ice-melting temperatures (Tm) of aqueous inclusions were measured using the thermal cycling method (Goldstein, 2001). The THMSG600 stage allows controlled heating and cooling rates from 0.01 °C to 150 °C/min, with high-precision Pt100 temperature sensors. Salinity (wt% NaCl equivalent) was calculated following Bodnar (1993). Measurement accuracy is ± 5 °C for Th and ± 0.1 °C for Tm.



4 Results and discussion

4.1 Source rock characteristics

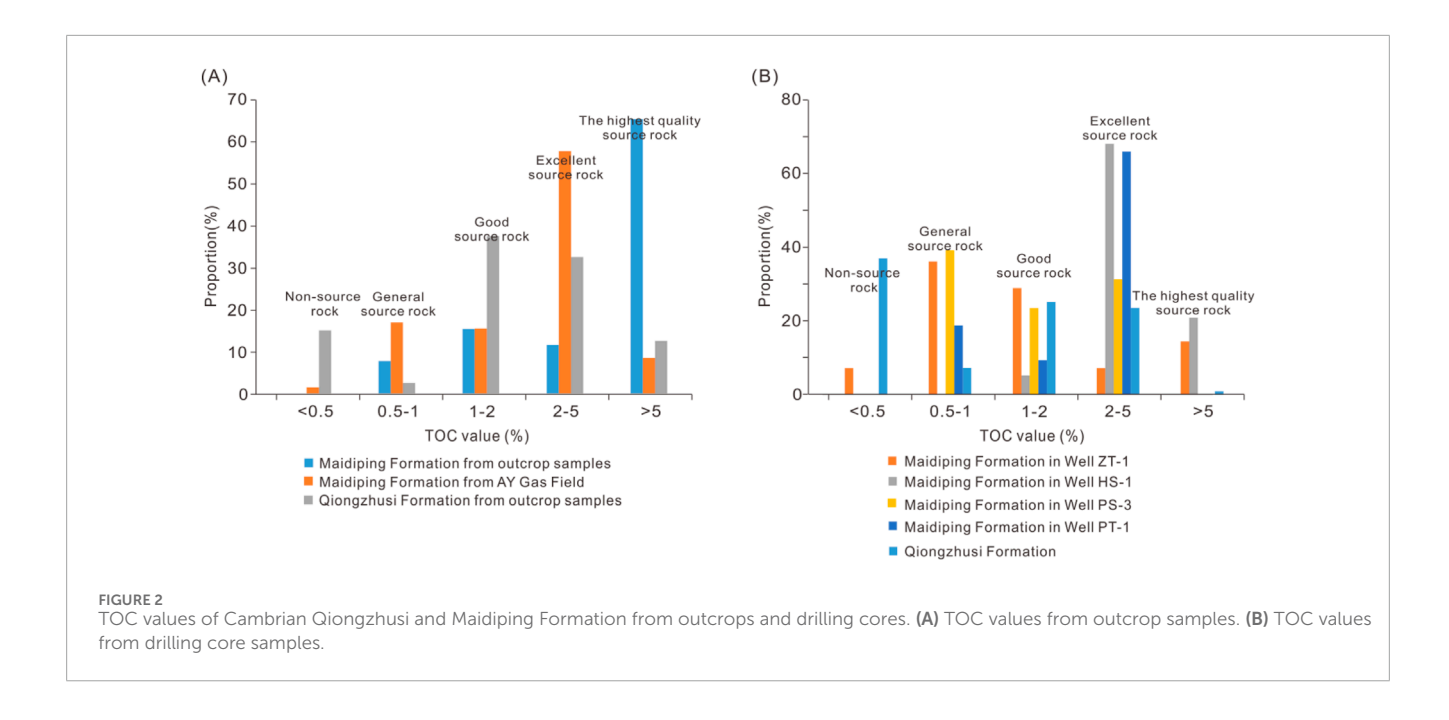
The TOC values of outcrop samples of source rocks from the Maidiping Formation in the western Sichuan Basin range from 0.70% to 22.68%, with an average of 2.95% (n = 26). The TOC values of Maidiping Formation source rocks from the North Sichuan Basin range from 0.16% to 6.83%, with an average of 2.53% (n = 40) (Figure 2A). Compared with the outcrop samples of the Qiongzhusi Formation, the Maidiping Formation source rocks have better quality (Figure 2B).

In response to the high degree of evolution of Lower Cambrian source rocks, microscopic component identification was applied to determine the type of kerogen (Pickel et al., 2017; Xu et al., 2021; Xu et al., 2025), as shown in Table 1. The sapropelite content of the nine outcrop samples of the source rocks in the Maidiping Formation ranges from 88% to 100%, with an average of 93%. The average content of exinite is 5.8%, while the content of vitrinite and inertinite is very low. The kerogen type index ranges from 89 to 100, with an average type index of 95.2. The kerogen type index of three Maidiping source rock samples from Well Z-4 ranges from 89.5 to 93, with an average type index of 94.8. It is suggested that the kerogen type of the Maidiping Formation is Type I (Cao, 1985; Dai et al., 1992). According to the rock pyrolysis data and bitumen reflectance data of five outcrop samples of Maidiping source rocks (Table 2), the maximum temperature (T_{max}) of rock pyrolysis is between 590 °C and 609 °C. The bitumen reflectance Rob is between 1.52% and 2.83%, indicating that the source rock has entered over-matured evolutionary stage (Dai et al., 1992; Hou and Liu, 2011).

The Qiongzhusi Formation shales are characterized by Type I organic matter, with kerogen δ^{13} C values ranging from -37‰ to -31‰, indicating a predominance of algal-derived material (Guo et al., 2024). Kerogen microscopy reveals that the organic matter is mainly composed of algal bodies, secondary bitumen, and solid kerogen, demonstrating good hydrocarbongenerating potential (Yong et al., 2024). Raman spectroscopy experiments further indicate that thermal maturity varies spatially under the influence of the Leshan-Longnvsi paleouplift: Ro values within the paleo-uplift range from 3.0% to 3.6%, corresponding to an appropriate thermal evolution stage, whereas outside the paleo-uplift, Ro values of 3.7%-4.2% indicate progression into the graphite stage (Chen et al., 2024). Laser-Raman measurements show equivalent vitrinite reflectance values of 3.30%-3.49%, confirming that the shales have reached the late overmature stage (Guo et al., 2024). Collectively, these characteristics suggest that the Qiongzhusi Formation shales possess high maturity and significant hydrocarbon-generation capability.

4.2 Genesis type of natural gas

Carbon isotopes are commonly used indicators for identifying the sources of natural gas, coal type gas, or oil type gas (Wei et al., 2015; Zheng et al., 2021). Due to the significant influence of thermal evolution on methane carbon isotopes, ethane carbon isotopes have become a commonly used effective indicator (Hou and Liu, 2011). Referring to identification chart for natural gas genesis types (Dai et al., 1992), the results show that the genesis types of natural gas in the Dengying Formation are relatively complex, including coal type gas, oil type gas, and a mixture of coal type gas and oil



type gas (Figure 3A). This result is obviously inconsistent with the actual geological background, as coal-bearing strata do not exist in the Ediacaran-Cambrian system in the South Sichuan Basin. This is because the identification chart is suitable for matured to highly matured natural gas, and is not suitable for identifying overmatured natural gas, especially the mixed products of oil-cracking gas and kerogen-cracking gas. The carbon isotope composition of natural gas is not only influenced by the type of parent material, but also by maturity. In the over-matured stage, accompanied by the generation of oil-cracking gas and kerogen-cracking gas, isotopic changes are greater (Hou and Liu, 2011). Zhao et al. (2021) proposed that the variation of $\delta^{13}C_2$ in natural gas from the Ediacaran-Cambrian system is not influenced by sulfate thermochemical reduction (TSR), but by the differences in the contribution ratios of source rocks of different maturity levels. Referring to the method proposed by Whiticar (1993) for classifying genesis types based on natural gas composition (C_1/C_{2+3}) and $\delta^{13}C_2$ (Whiticar, 1999), the results show that the natural gas in the Dengying Formation comes from a mixture of crude oil cracking gas and kerogen cracking gas (Figure 3B).

In order to further determine the ratio of crude oil cracking gas and kerogen cracking gas, the method proposed by Zhang et al. (2018) was used to identify the mixture ratio of over-matured kerogen-cracking gas (Ro \geq 2.5%) and oil-cracking gas of different maturities. The calculation formula is as follows:

$$\delta^{13}C_{i}(\%_{0}) = \frac{P_{k} \times x_{i} \times \left(1000 + \delta^{13}C_{i,k}\right) + P_{o} \times y_{i} \times \left(1000 + \delta^{13}C_{i,o}\right)}{P_{k} \times x_{i} + P_{o} \times y_{i}} - 1000$$
(1)

In Formula 1, x_i and y_i represents the molar percentage content of hydrocarbon components (C_i) in kerogen-cracking gas and oil-cracking gas, respectively $(0 \le x_i, y_i \le 1)$; $\delta^{13}C_{i,k}$ and $\delta^{13}C_{i,o}$ represents $\delta^{13}C$ of hydrocarbon components (C_i) in kerogen-cracking gas and oil-cracking gas, respectively. P_k and P_o are the mixing ratios of

kerogen-cracking gas and oil-cracking gas, respectively. The natural gas sources of the Dengying Formation vary in different areas, but the genesis type of natural gas is all oil-cracking gas. The natural gas in Dengying Formation second Member in AY Gas Field is mainly composed of oil-cracking gas (Figure 3C), while most wells in Dengying fourth Member are mainly composed of oil-cracking gas. Oil-cracking gas accounts for approximately 60% of the natural gas in the Well PT-1. However, the Dengying Formation of WY Gas Field is mainly composed of kerogen-cracking gas, accounting for about 60%.

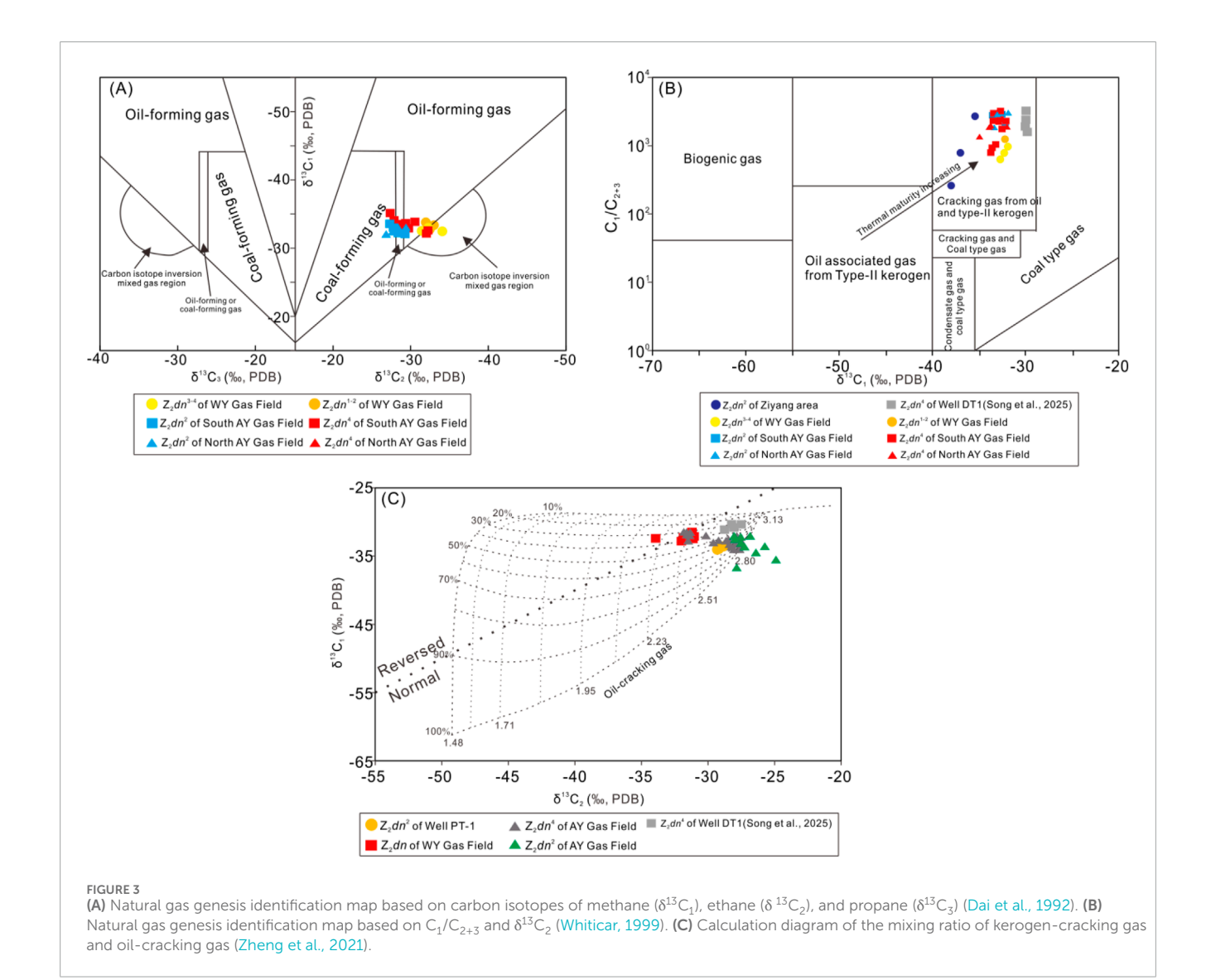
Song et al. (2025) suggested that natural gas in the Dengying Formation on both the eastern and western sides of the rift trough is dominantly oil-cracking gas. Similarly, Fan et al. (2022) reported that the AY Gas Field is mainly charged by oil-cracking gas, which is consistent with our findings. From a geological perspective, the main source rocks of the Cambrian Qiongzhusi Formation experienced shallow burial in the early stage, followed by rapid deep burial during the Late Triassic-Cretaceous. This burial history drove organic matter evolution into a gas-dominated stage. By the end of the Cretaceous, formation temperatures peaked, marking the critical period for oil cracking and gas accumulation (Shuai et al., 2023; Guo et al., 2024; Wang et al., 2024). Shuai et al. (2023) further highlighted regional differences, noting that the Ziyang area, located in structural highs, was favorable for both oil accumulation and subsequent oil-cracking gas preservation within lithologic-structural traps. In contrast, areas such as AY Gas Field, WY Gas Field and Yongchuan area, though also charged by oil and oil-cracking gas, experienced significant late-stage gas loss. In these areas, ultra-late gas release from Qiongzhusi shales provided crucial supplementary charge, ensuring high gas productivity. These insights are consistent with our conclusions on gas origins. Moreover, in the AY Gas Field, condensate shows much greater abundance and extent than normal crude oil, and its secondary cracking has supplied widely distributed gas in Dengying reservoirs (Shuai et al., 2023).

TABLE 1 Microscopic composition and type classification of kerogen in Maidiping Formation source rocks.

Туре	I	I	I	I	Ι	I	Ι	I	Ι	I	I	Ι
Type index	100	95	93	94	68	97	94	97	86	89.5	93.0	93.0
Inertinite	0	1	0	0	0	1	1	1	П	0	0	0
Euvitrinite	0	2	1	0	0	1	1	0	1	0	0	0
Provitrinite	0	0	1	0	0	1	1	0	0	9	4	4
Humus acidus	0	0	0	0	0	0	0	0	0	0	0	0
Planktonic algal body Humus acidus	0	2	9	12	14	2	3	1	12	0	0	0
Sapropelic amorphous body	100	96	92	88	98	95	94	86	88	94	96	96
Source Sample ID	4-1D	6-1D	11-1D	34-3D	35-2D	36-2D	40-3D	45-1D	54-2D	4236.8 m	4277.94 m	4305 m
Source	Outcrop						Well Z-4					

TABLE 2 Organic matter pyrolysis results of outcrop source rocks in Maidiping Formation.

Sample ID	Lithology	TOC(%)	Chloroform bitumen "A" (ppm)	S ₁ +S ₂ (%)	T _{max} (°C)	Rob (%)	Kerogen type
4-1D	Black shale	42.68	37.12	0.26	606	2.83	I
11-1D	Black shale	7.29	111.82	1.02	605	1.79	I
34-3D	Black shale	11.44	51.75	0.53	590	2.62	I
45-1D	Black shale	5.76	59.83	0.14	609	2.78	I
54-2D	Phosphorous siliceous rock	0.75	10.64	0.03	590	1.52	I



4.3 Source of natural gas

4.3.1 Carbon isotope characteristics

Carbon isotopes of natural gas or kerogen are commonly used for gas source comparison (Chang et al., 2022). As shown in Figure 4A, the $\delta^{13}C_{\rm kerogen}$ distribution of Dengying mudstone

samples ranges from -34.5% to -28.1%, with an average of -31.2%, exhibiting typical characteristics of sapropelic kerogen (n = 31). The distribution of $\delta^{13}C_{kerogen}$ in Qiongzhusi shale samples (n = 60) ranges from -36.8% to -29.9%, with an average of -32.8%, slightly lower than that of the Dengying Formation, exhibiting typical characteristics of sapropelic kerogen as well (Hou and Liu,

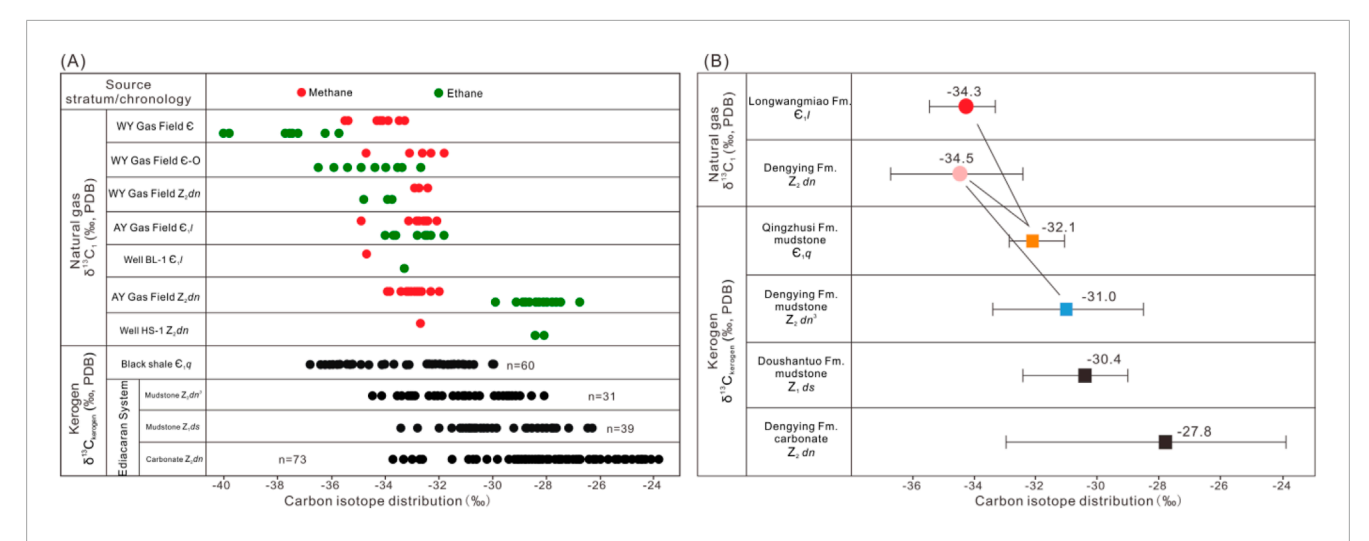


FIGURE 4
(A) Carbon isotope distribution map of natural gas and kerogen (modified from Wei et al., 2015), (B) Comparison of methane carbon isotopes between kerogen from different source rocks and Longwangmiao and Dengying natural gas in AY Gas Field.

2011). The distribution of $\delta^{13}C_{kerogen}$ in Doushantuo mudstone samples (n = 39) ranges from -33.6‰ to -26.3‰, with an average of -29.6‰, slightly larger than that of the Dengying Formation, exhibiting typical characteristics of sapropelic kerogen as well. The distribution of $\delta^{13}C_{kerogen}$ in Dengying Formation carbonate samples (n = 73) ranges from -33.1‰ to -23.8‰, with an average of -27.8‰, slightly larger than that of the mudstone mentioned above.

Overall, the Qiongzhusi Formation has the lightest $\delta^{13}C_{kerogen}$ (Figure 4A). According to the carbon isotope fractionation of hydrocarbon generation, the natural gas of Longwangmiao Formation in WY Gas Field and the natural gas of Ediacaran in WY Gas Field, which have significantly lighter isotopes, may originate from the Qiongzhusi source rocks. The $\delta^{13}C_{kerogen}$ of the Doushantuo mudstone, Dengying mudstone, and carbonate rock samples in the Ediacaran system is relatively heavy, and is similar to the $\delta^{13}C_1$ and $\delta^{13}C_2$ of the Dengying Formation in the AY Gas Field and Yongchuan area, showing obvious affinity (Figure 4A). Similarly, the natural gas in Longwangmiao Formation of AY Gas Field and Well BS-1 mainly comes from the Qiongzhusi Formation source rocks

From kerogen to crude oil and from bitumen to methane, δ^{13} C becomes increasingly lighter, producing a fractionation degree of 2‰–4‰, especially $\delta^{13}C_{kerogen}$ which can only be heavier than $\delta^{13}C_1$ (Hou et al., 2021). The carbon isotope fractionation of kerogen from the Qiongzhusi Formation (\mathcal{E}_1q) and methane from the Longwangmiao Formation (ϵ_1) is 2‰–3‰ (Figure 4B), indicating that the gas source comes from the Qiongzhusi Formation. The carbon isotope fractionation degrees of kerogen from Dengsan Formation, Qiongzhusi Formation, and natural gas methane from Dengying Formation are 3.48%-2.38%, respectively, suggesting that they are all gas sources of Dengying Formation. The methane carbon isotope fractionation of Doushantuo mudstone, Dengying carbonate rock, and Dengying Formation natural gas are all greater than 4%, with values of 4.48% and 6.68%, respectively. It is suggested these two source rocks are not the gas source rocks of the Dengying Formation.

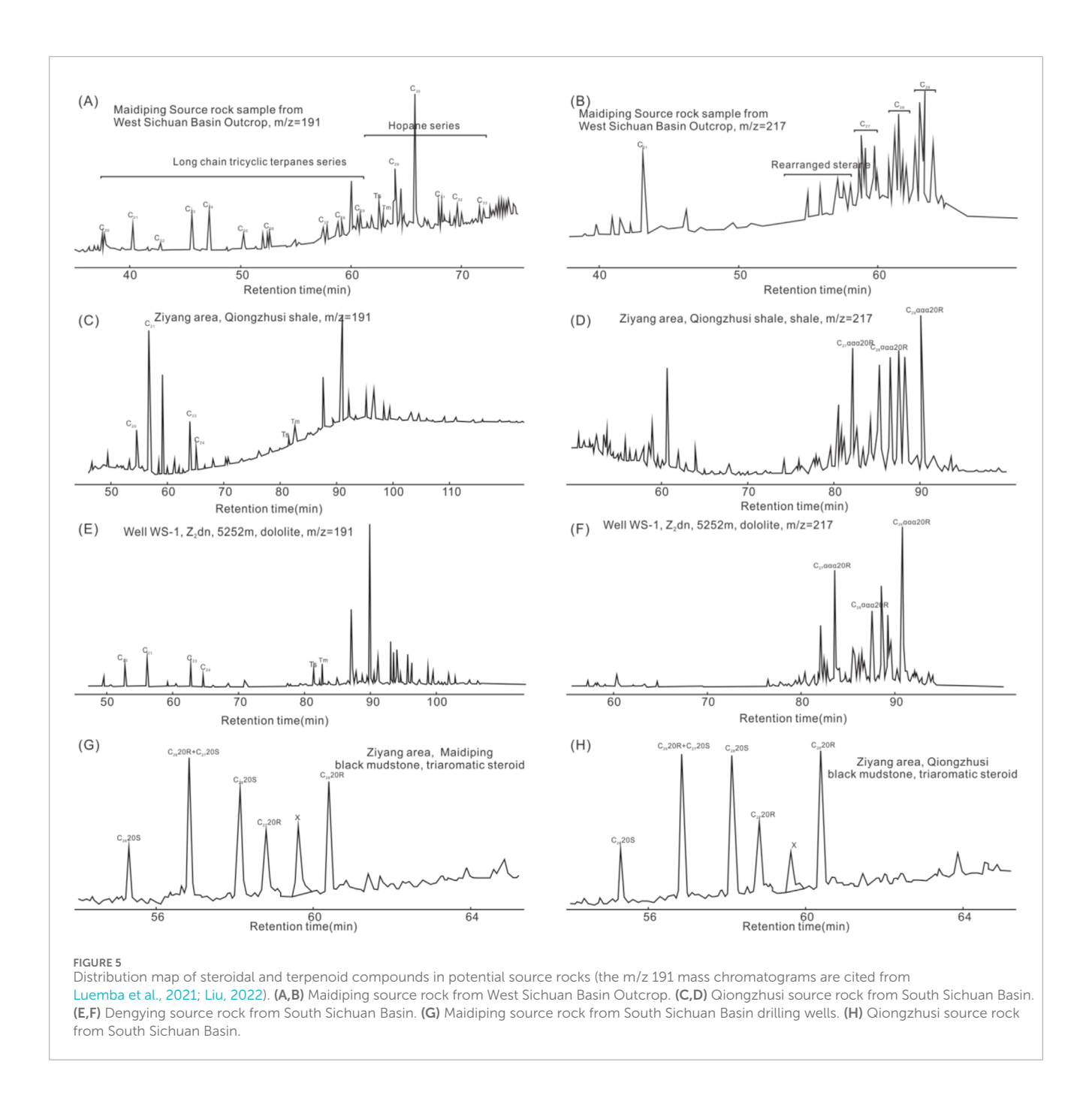
4.3.2 Comparison of biomarker compounds

Due to the simple composition of natural gas, there is relatively little effective information available for gas source tracking. Therefore, biomarker compounds are an important method for oil and gas sources (Sun et al., 2019). The distribution characteristics of biomarker compounds in different source rocks or reservoir bitumen have significant differences, laying the foundation for gas source comparison research (Chen et al., 2017; Fang et al., 2024).

4.3.2.1 Biomarker compounds of source rocks

The tricyclic terpenoids in the source rocks of Maidiping are distributed between C_{19} and C_{29} , with C_{23} being the dominant group. They mainly display a $C_{19} < C_{20} < C_{21}$ distribution pattern and a reverse "V"-shape of $(C_{20}, C_{21}$ and $C_{23})$ (Figure 5A). The carbon number distribution of pentacyclic triterpenoids with a hopane structure as the skeleton is mostly concentrated in the range of C_{27} to C_{33} , with C_{30} hopane as the main peak. Ts > Tm, and the C_{29} rearranged hopane content is high. In the C_{31} - C_{35} series, the content of C_{31} - C_{34} slightly decreases with the increase of carbon atoms. The main steroids are regular steroids $(C_{27}$ - $C_{29})$ and rearranged steroids $(C_{27}$ - $C_{29})$, followed by pregnane and a small amount of 4-methylsteroids. In regular steroids, C_{29} is slightly higher than C_{27} (or similar) and significantly higher than C_{28} , exhibiting a "V" - shaped distribution pattern (Figure 5B).

The carbon atom number distribution of tricyclic terpenoids in the Qiongzhusi source rocks ranges from C_{19} to C_{29} , with most samples dominated by C_{20} . C_{21} , C_{23} , and C_{23} exhibit a clear inverted "V"-shape distribution (Figure 5C). The pentacyclic triterpenoids with hopane structure as the skeleton are distributed from C_{27} to C_{35} , with C_{30} hopane as the main peak. The characteristic of Tm being greater than Ts is significantly different from the source rocks of the Maidiping Formation. In the distribution of steroids, regular steroids (C_{27} - C_{29}) and rearranged steroids (C_{27} - C_{29}) are predominant, followed by pregnane. The distribution of regular steranes differs significantly from the source rocks of the Maidiping Formation, showing an inverted "L"-shaped distribution,



with C_{29} showing a clear advantage and C_{27} slightly larger than C_{28} (Figure 5D).

The tricyclic terpenoids in Dengying dolomite are distributed between C_{19} and C_{29} , with C_{21} showing a slight predominance of C_{21} (Figure 5E). C_{20} , C_{21} , and C_{23} show an inconspicuous inverted "V"-shaped pattern, which is similar to that of the Qiongzhusi shales (or mudstone) (Figure 5C). The pentacyclic triterpanes with a hopane skeleton are mainly distributed between C_{27} and C_{35} , dominated by C_{30} hopane, followed by C_{29} rearranged hopane, showing a typical Tm > Ts feature. This contrasts markedly with the Ts > Tm characteristic of the Maidiping source rocks (Figure 5A). Regarding sterane distribution, the major components are regular steranes (C_{27} - C_{29}) and rearranged

steranes (C_{27} - C_{29}), with pregnanes as secondary constituents. The distribution of regular steranes resembles that of the Qiongzhusi source rocks, showing an inverted "L"-shaped pattern (Figure 5F). Specifically, C_{29} is strongly dominant, whereas in the Dengying source rocks, C_{27} is significantly higher than C_{28} (Figure 5E).

In terms of triaromatic sterane distribution, an unknown X peak occurs in both the Maidiping and Qiongzhusi formations. However, in the Maidiping Formation, $C_{27}20R$ is slightly lower than the X peak (Figure 5G), whereas in the Qiongzhusi Formation, $C_{27}20R$ is clearly higher than the X peak (Figure 5H). This directly indicates significant differences between the Maidiping and Qiongzhusi source rocks.

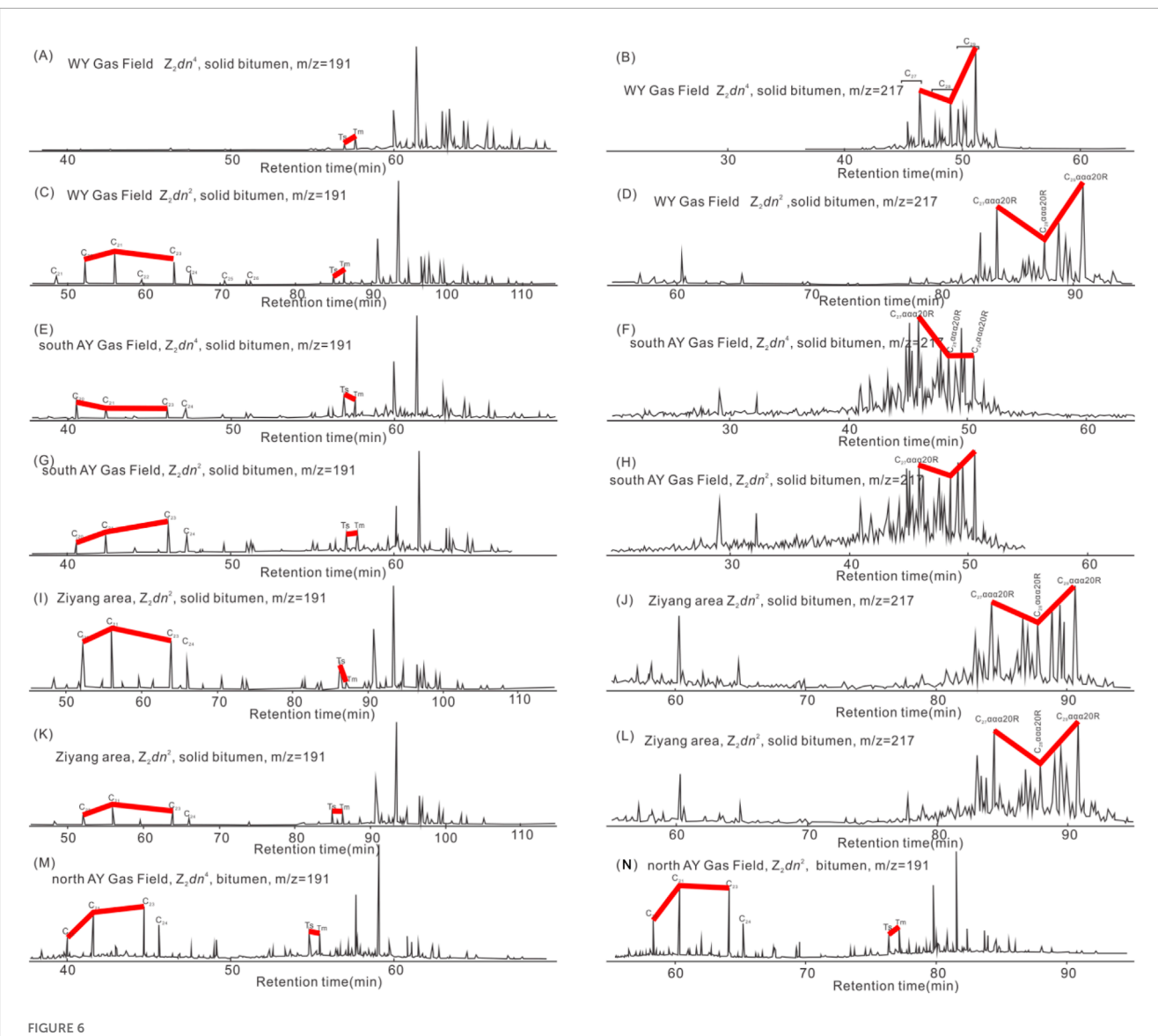


FIGURE 6 (A,B) Distribution of bitumen steranes (m/z = 217) and terpenes (m/z = 191) in the Dengying Formation reservoir of WY Gas Field. (C,D) Distribution of bitumen steranes (m/z = 217) and terpenes (m/z = 191) in the Dengying Formation reservoir of WY Gas Field. (E,F) Distribution of bitumen steranes (m/z = 217) and terpenes (m/z = 191) in the Dengying Formation reservoir of south AY Gas Field. (G,H) Distribution of bitumen steranes (m/z = 217) and terpenes (m/z = 191) in the Dengying Formation reservoir of south AY Gas Field. (I,J) Distribution of bitumen steranes (m/z = 217) and terpenes (m/z = 191) in the Dengying Formation reservoir of Ziyang area. (K,L) Distribution of bitumen steranes (m/z = 217) and terpenes (m/z = 191) in the Dengying Formation reservoir of Ziyang area. (M) Distribution of bitumen terpenes (m/z = 191) in the Dengying Formation reservoir of north AY Gas Field. (N) Distribution of bitumen terpenes (m/z = 191) in the Dengying Formation reservoir of north AY Gas Field.

4.3.3 Biomarker compounds of reservoir bitumen

In the WY Gas Field, the bitumen in the Dengying fourth Member reservoirs contains a low abundance of tricyclic terpanes. The pentacyclic triterpanes are mainly distributed between C_{27} and C_{35} , with C_{30} hopane as the dominant peak, accompanied by notable amounts of C_{29} norhopane and C_{29} T, and characterized by Tm > Ts (Figure 6A). Regular steranes display a distribution of $C_{29} > C_{27} > C_{28}$ in an inverted "L" pattern, with no obvious predominance of C_{27} over C_{28} (Figure 6B). Both features are consistent with the Qiongzhusi source rocks, indicating a significant contribution of the Qiongzhusi source rocks to gas accumulation in the Dengying fourth Member of the WY Gas Field.

In the bitumen of the Dengying second Member reservoirs of the WY Gas Field, tricyclic terpanes range from C_{19} to C_{29} , with C_{21} slightly dominant (Figure 6C). C_{20} , C_{21} , and C_{23} show a weak inverted "V" distribution. Pentacyclic hopanes are dominated by C_{30} hopane with Tm > Ts (Figure 6C). These features are similar to both the Qiongzhusi and Dengying source rocks. Regular steranes display a weak inverted "L" pattern, with C_{27} significantly higher than C_{28} (Figure 6D). These characteristics suggest that, in addition to the Qiongzhusi source rocks, the Ediacaran Dengying source rocks also contributed to gas accumulation in the Dengying second Member of the WY Gas Field.

In the South AY Gas Field, the bitumen from Well GS-1 in the Dengying fourth Member reservoirs is dominated by

 $\rm C_{20}$ tricyclic terpane, showing a weak "V"-shaped distribution (Figure 6E). Pentacyclic hopanes peak at $\rm C_{30}$, followed by $\rm C_{29}$, with Ts significantly higher than Tm, consistent with the Maidiping source rocks (Figure 5A). However, the regular sterane distribution is dominated by $\rm C_{27}$, with $\rm C_{28}$ and $\rm C_{29}$ nearly equal, showing a clear "L"-shaped pattern (Figure 6F). These features are not entirely consistent with any single source (Qiongzhusi mudstones, Dengying dolostones, or Maidiping source rocks), but show higher similarity to the Maidiping mudstones, which also display a strong $\rm C_{27}$ dominance in sterane distribution. Therefore, we infer that the gas in the Dengying fourth Member of Well GS-1 is mainly sourced from the Maidiping Formation.

In the Dengying second Member reservoirs of Well GS-1, tricyclic terpanes are dominated by C_{23} , with $C_{20} < C_{21} < C_{23}$, forming a weak inverted "V" pattern (Figure 6G). Pentacyclic hopanes are distributed from C_{27} to C_{35} , with C_{30} as the main peak and C_{29} secondary, showing Ts slightly lower than Tm, consistent with the Maidiping source rocks (Figure 5A). However, the regular sterane distribution shows an inverted "L" pattern, with C_{29} predominance and C_{27} slightly higher than C_{28} (Figure 6H), which resembles the Qiongzhusi source rocks (Figure 5D). Thus, we propose that the gas in the Dengying second Member of Well GS-1 is likely derived from a mixture of the Qiongzhusi and Maidiping source rocks.

In the Ziyang area, bitumen from the Dengying second Member reservoir of Well Z-1 is characterized by a slight dominance of C21 tricyclic terpanes (Figure 6I), showing a weak inverted "V" shaped distribution, similar to that of the Dengying source rocks. Pentacyclic triterpanes are dominated by C_{30} hopane, with Ts > Tm (Figure 6I), comparable to the Maidiping Formation source rocks. Regular steranes display an inverted L-shaped distribution, with C₂₇ significantly exceeding C₂₈ (Figure 6J), closely resembling that of the Dengying source rocks. These features indicate that natural gas in Well Z-1 (Ziyang area) is of mixed-source origin, mainly derived from the Maidiping Formation source rocks, with minor input from Dengying Formation dolomite. In Well Z-6 (Ziyang area), the Deng second Member reservoir shows tricyclic terpane and regular sterane distributions resembling those of the WY Gas Field and Ziyang area (Figures 6K,L), but with Ts values approximating Tm. This also suggests a mixed-source origin, with natural gas primarily sourced from the Qiongzhusi Formation.

The tricyclic terpenes in the bitumen of the Dengying fourth Member and second Member reservoirs in the Northern AY Gas Field are distributed in the range of C_{19} to C_{29} , and the pentacyclic triterpenoids are distributed in the range of C_{27} to C_{35} . C_{30} hopane is the main peak, followed by C_{29} reduced hopane. The tricyclic terpenes in the Dengying fourth Member are mainly C_{23} , with Ts > Tm (Figure 6M), suggesting that natural gas mainly originates from the Maidiping Formation. C_{21} has a slight advantage in the tricyclic terpenes of the Dengying second Member of Northern AY Gas Field (Figure 6N), with Ts < Tm, suggesting that it originates from the Qiongzhusi source rock, but there are also other natural gas mixtures.

For the distribution of triaromatic steranes, the X peak was detected in the bitumen of the Dengying Formation in Ziyang area, and Southern Sichuan Basin, showing $C_{27}20R > X$ peak (Figures 7A–C). The natural gas in the WY Gas Field and the Dengying Formation in Ziyang area is mainly contributed by the

Qiongzhusi source rock, with limited supply from the Maidiping source rock. The content of X peak in the Southern Sichuan Basin is very low (Figures 7D,E), and even some sample does not contain X peak, suggesting that it may be related to the source rocks of the Ediacaran carbonate rocks (Figures 7D,F).

In summary, based on the comparison of solid bitumen and source rocks, the natural gas in the Ediacaran Dengying Formation of WY Gas Field mainly comes from the Qiongzhusi source rock. However, the natural gas sources in Ziyang area and AY Gas Fields are complex, and different wells or members may have different sources and ratios of natural gas supply, indicating that the Qiongzhusi, Maidiping, and Ediacaran source rocks all contribute to natural gas accumulation.

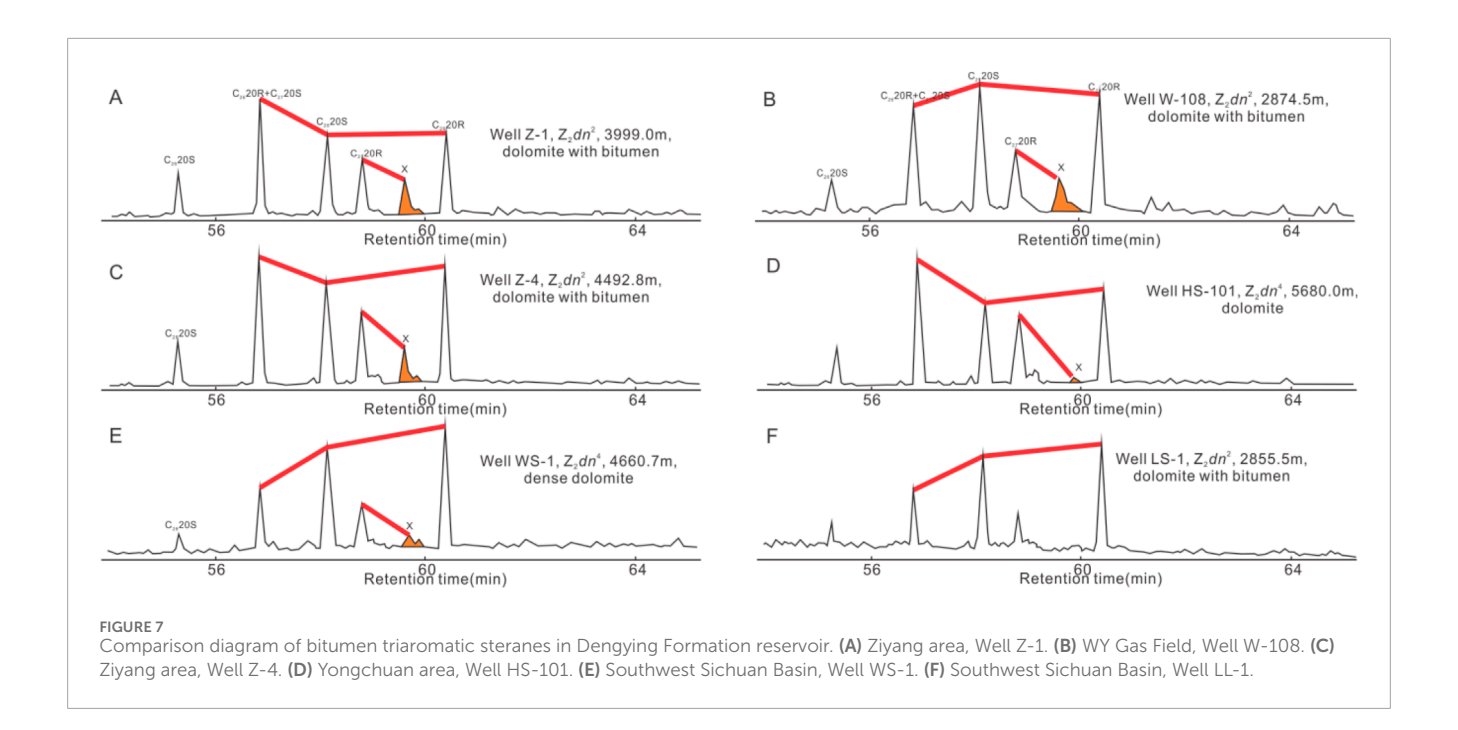
4.4 Hydrocarbon charging processes

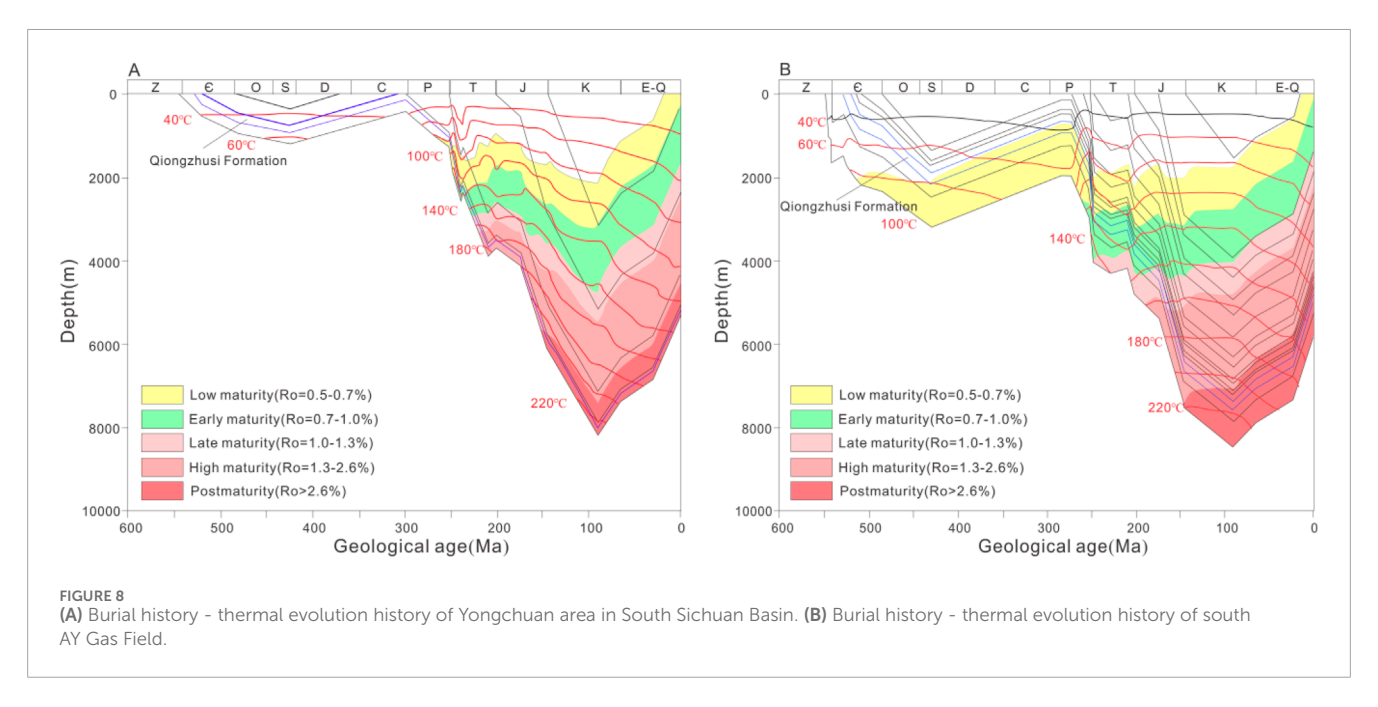
4.4.1 Hydrocarbon generation evolution

The key influencing factors of hydrocarbon generation in source rocks are time and temperature, and the simulation of hydrocarbon generation history is based on the burial history and thermal history of source rocks (Liu et al., 2018). The Basin Mod software was used to simulate the hydrocarbon generation history of Yongchuan area and Anyue area (Figures 8A,B). Firstly, the burial history of the strata was reconstructed based on the sedimentary and tectonic evolution process of the basin. Then, assuming a paleo-geothermal gradient model (thermal history evolution model), combined with the burial history of the source rocks, the paleo-geothermal model experienced by the source rock interval is calculated, and the corresponding geothermal history isotherms are established. By using the dynamic model of R_O evolution and thermal evolution history, R_O of each source rock is calculated, and measured Ro values are constrained and calibrated to improve the accuracy of settlement results, thus obtaining a paleo-geothermal gradient and thermal history model suitable for the study area. Finally, the Loptain TTI method was used to simulate R_O variation in source rocks over time, and to determine the relationship between organic matter maturity time and depth temperature. The evolution stages of organic matter hydrocarbon generation were divided, and the inversion of the hydrocarbon generation history of Cambrian source rocks was achieved under the constraint of the representative R_O depth relationship in the area.

At the end of the Silurian period, the Qiongzhusi source rocks in the southwestern Sichuan Basin were in the immature evolution stage (Figure 8A), and the thermal evolution degree of the Qiongzhusi source rocks gradually increased towards the eastern part of the basin. The $\rm R_{\rm O}$ of Qiongzhusi source rocks in the South AY Gas Field is around 0.6%–0.7%, and it has begun to enter the oil-generation window (Figure 8B). The Well HS1 inside the intracratonic sag has entered the early stage of maturity $^{\rm l}$. In the Middle to Late Permian, the Qiongzhusi source rocks in the southwestern part of the basin began to enter a low maturity evolution stage, while the Qiongzhusi source rocks in the South

¹ Shi, C. H. (2017). Correlation of atmospheric hydrocarbon source evolution in Sinian-Lower Cambrian in Sichuan Basin. Nanjing: Nanjing University. Unpublished master's thesis.





AY Gas Field and the intracratonic sag had all entered the oil-generation window and reached the oil-generation peak. At the end of the Triassic-Jurassic, the Indosinian-Yanshan Movement caused significant deep burial of the Lower Paleozoic source rocks in the basin. The Qiongzhusi source rocks in the South AY Gas Field and the intracratonic sag entered over-matured stage, mainly composed of kerogen-cracking gas and oil-cracking gas. At the end of the Early Cretaceous, the distribution pattern of the thermal evolution degree of the Qiongzhusi source rock is basically similar to today, indicating that hydrocarbon generation has basically stopped since the Late Cretaceous (Shi, 2017). Since the end of the Cretaceous, except for the Leshan area in southwestern Sichuan, the Ro of the Cambrian Qiongzhusi source rocks has been above 2.0%,

reaching the oil-cracking stage. The thermal evolution degree of the Qiongzhusi source rocks in the southwest of the basin is the lowest, gradually increasing towards the southeast, especially in areas such as Changning, Luzhou, and Yongchuan where the $\rm R_{\rm O}$ of the source rocks is above 4.6% (Deng et al., 2024; Shuai et al., 2023). Overall, the Qiongzhusi source rock entered the oil-generation period from the Late Silurian to the end of the Late Cretaceous tectonic uplift. Therefore, the oil-generation period of the Qiongzhusi source rock spans across the Devonian, Carboniferous, Permian, Triassic, and Jurassic periods, with the Permian and Triassic being its main oil-generation periods. The gas-generation period lasted from the Late Permian to the end of the Early Cretaceous, with the Jurassic being the main gas-generation period.

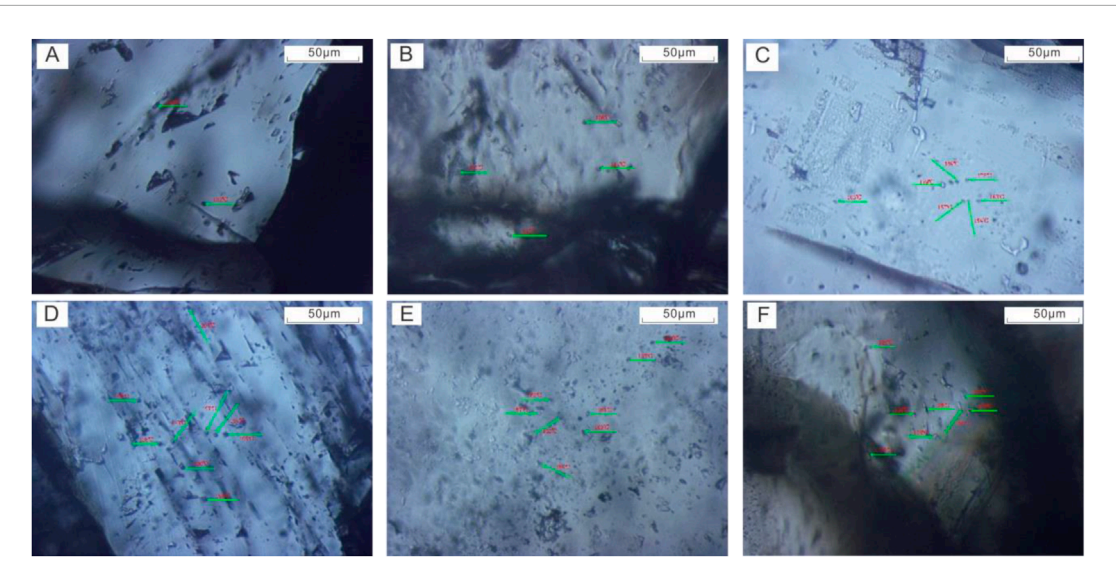


FIGURE 9
Microscopic characteristics of fluid inclusions in the Dengying Formation reservoir in South Sichuan Basin. (A) Well Z-4, Z_2dn_2 , 4484 m, vapor-liquid inclusion. (B) Well Z-6, Z_2dn_2 , 3758.31m, vapor-liquid inclusion. (C) Well Z-6, Z_2dn_2 , 3716m, vapor-liquid inclusion. (D) Well Z-1, Z_2dn_2 , 3557.6m, vapor-liquid inclusion. (E) Well W-117, Z_2dn_2 , 3177.65m, vapor-liquid inclusion. (F) Well W-113, Z_2dn_2 , 3128.76m, vapor-liquid inclusion.

4.4.2 Charging period of natural gas

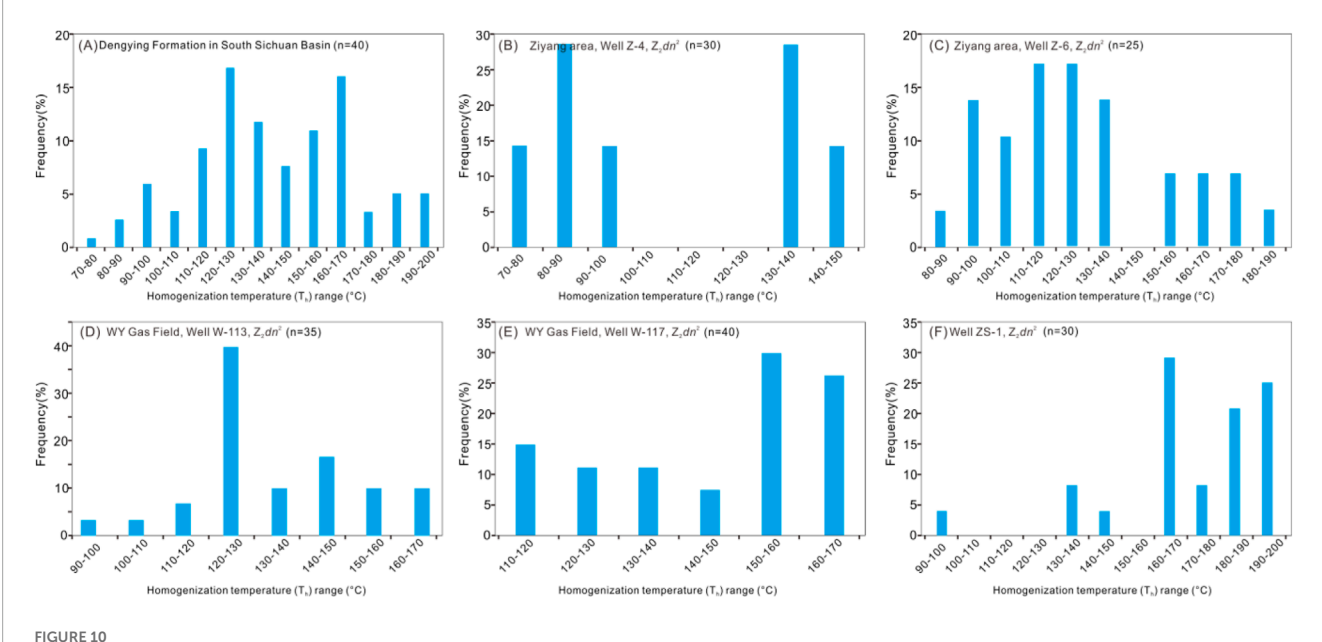
Hydrocarbon-containing inclusions are defined as the gas, liquid, or solid bitumen captured during the crystallization of minerals such as carbonates and quartz during the primary or secondary migration of hydrocarbons in the post-diagenetic stage (Deng et al., 2024; Xie et al., 2023). The hydrocarbon-containing inclusions in the Dengying Formation reservoir are developed in multi-stage dolomite cement in fractures and vugs (Figure 9). Under the microscope observation and microthermometry results indicate that four types of inclusions were captured in the Dengying Formation reservoir, including saline inclusions, vapor-liquid inclusion, oil-containing inclusions and hydrocarbon-containing inclusion composed of bitumen, oil, and natural gas.

The T_h and petrological characteristics of inclusions reflect the formation of early-stage paleo-oil pools and the process of oil-cracking to form natural gas in the Dengying Formation (Luo et al., 2024). By measuring the phase, color, and temperature of the inclusions, the paleo-temperature changes during the formation of hydrocarbons can be reflected. A large number of inclusions were found in the cement of the Dengying Formation reservoir at different stages, suggest continuous hydrocarbon charging. In the early-stage dolomite, the inclusions were mainly heavy oil-inclusions, while in the later stage cement, the content of light oil-inclusions and gas-inclusions gradually increased, and the T_h of inclusions increased.

The distribution of T_h values in the Dengying Formation of Southern Sichuan Basin ranges from 70 °C to 200 °C, with peak values of 120 °C–130 °C and 160 °C–170 °C, respectively (Figure 10A). The T_h distribution in different tectonic zones varies to some extent. The T_h in the inclusions of Well Z-4 in Ziyang area is relatively low, distributed between 70 °C and 150 °C, showing two peak ranges of 80 °C–90 °C and 130 °C–140 °C (Figure 10B). The Well Z-6 is located on the west side of the intracratonic sag, and the T_h distribution of the inclusions is between 80 °C and

190 °C, showing two peak areas of 90 °C–100 °C and 110 °C–140 °C (Figure 10C). The T_h distribution of inclusions in Well W-113 of WY Gas Field is between 80 °C and 170 °C, showing a single peak interval of 120 °C–130 °C (Figure 10D). The T_h distribution in Well W-117 of WY Gas Field is between 110 °C and 170 °C, showing a single peak area between 150 °C and 170 °C (Figure 10E). The T_h in Well ZS-1 is relatively high, and the proportion of low-temperature inclusions is relatively small (Figure 10F). The differences in spatial distribution and tectonic movements of source rocks in different areas lead to variations in the maturation process of source rocks. This will result in significant differences in Th values across different areas. Meanwhile, the alteration of external hydrothermal fluids has resulted in differences in Th values among samples from different wells in the same area (Figure 10).

Based on the variation of Th and combined with the thermal evolution history of source rocks, the hydrocarbon charging periods of the Dengying Formation reservoir in Southern Sichuan Basin have been summarized. (1) The hydrocarbon-containing inclusions captured during the paleo-oil pool stage: From the Early Cambrian to the end of the Silurian, the Qiongzhusi source rocks gradually reached the hydrocarbon generation threshold, initiating expulsion and charging processes. Early liquid hydrocarbons migrated into the reservoirs and were trapped, forming the first generation of inclusions. These inclusions formed prior to the Permian. Statistical analysis indicates that dark brown or gray-brown liquid hydrocarbon inclusions account for approximately 90%, while gas-liquid inclusions make up only about 10%. In gas-liquid inclusions, the gas-to-liquid ratio is low, generally around 1%, and T_h mainly range from 70 °C to 120 °C. Due to the Caledonian and Hercynian tectonic movements, uplift and erosion occurred, terminating hydrocarbon generation and limiting the scale of liquid hydrocarbon charging (Shuai et al., 2023; Deng et al., 2025). (2) Vapor-liquid inclusions captured during the formation stage of paleo-oil and gas pools: During the Middle to Late Triassic, the



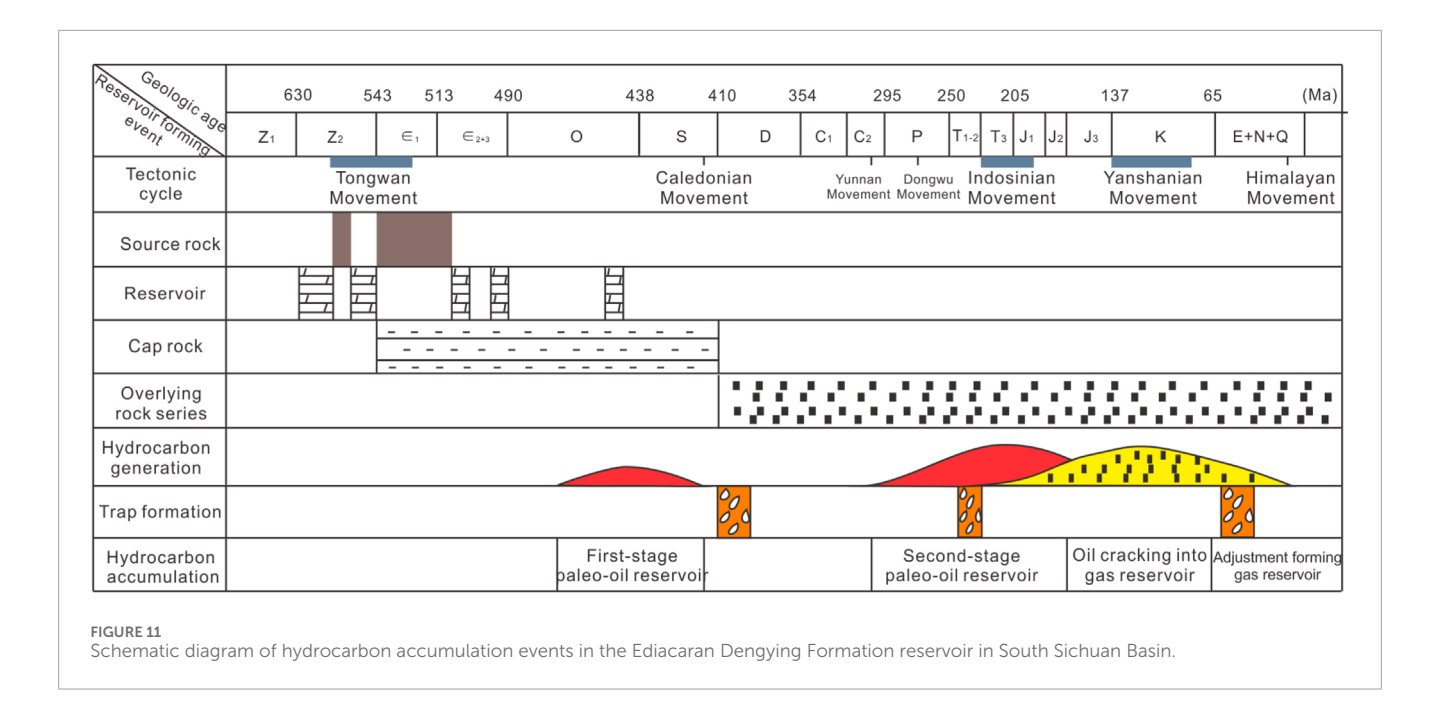
Homogenization temperature (Th) distribution frequency histogram of fluid-inclusions in Dengying Formation reservoir. (A) Th distribution frequency histogram of fluid-inclusions in Dengying Formation of South Sichuan Basin. (B) Th distribution frequency histogram of fluid-inclusions in Dengying 2nd Member of Well Z-4. (C) Th distribution frequency histogram of fluid-inclusions in Dengying 2nd Member of Well Z-6. (D) Th distribution frequency histogram of fluid-inclusions in Dengying 2nd Member of Well W-113 in WY Gas Field. (E) Th distribution frequency histogram of fluid-inclusions in Dengying 2nd Member of Well W-117 in WY Gas Field. (F) Th distribution frequency histogram of fluid-inclusions in Dengying 2nd Member of Well X-1.

Sichuan Basin entered the foreland basin evolution stage. The Qiongzhusi Formation underwent rapid burial and heating, with organic matter reaching a high maturity stage. Large volumes of liquid and gaseous hydrocarbons were generated and charged into reservoirs, where fluid inclusions commonly occur in clusters or bands within dolomite cement filling dissolution pores. Among these inclusions, gray-brown gas-liquid hydrocarbons (including hydrocarbon brine) account for 10%-80%, with gas-liquid ratios of 2%-10%, and T_h ranging from 120 °C to 170 °C. Gas-liquid inclusions dominate this stage. The homogenization temperature range of these inclusions overlaps with that of the paleo-oil pool stage, indicating that hydrocarbon charging in some locations was a continuous process. (3) Bitumen-containing inclusions and methane-containing inclusions captured during the cracking stage of paleo-oil pools: From the Jurassic to the Early Cretaceous, the Qiongzhusi source rocks entered a high to over-mature stage. Earlyformed liquid hydrocarbons and kerogen underwent extensive cracking to gas, generating bitumen and large-scale gas pools. Multiple types of gaseous hydrocarbons entered the reservoirs in large volumes and were trapped as gas inclusions. These inclusions occur in clusters or bands within crystalline dolomite filling dissolution pores, but their abundance is lower than that of the previous two stages. Gas inclusions dominate, with high gas-toliquid ratios and T_h of 150 °C-200 °C. The gaseous hydrocarbon inclusions are primarily CH₄, with minor liquid hydrocarbon inclusions and bitumen. According to the history of hydrocarbon charging, the paleo-oil pool in the Dengying second Member of Ziyang area was formed in the Silurian period, while the oilcracking and charging period in the Dengying Formation of AY Gas Field occurred between the Late Jurassic and Cretaceous periods.

4.4.3 Evolution and model of hydrocarbon charging

The complex tectonic environment of the Sichuan Basin determines the complexity of hydrocarbon accumulation in the Dengying Formation. After the formation of early paleo-oil and gas pools, they inevitably underwent multiple tectonic movements and were accompanied by the destruction and adjustment (Whiticar, 1999). The main accumulation events experienced by the Dengying Formation reservoir in the Sichuan Basin are shown in Figure 11. Affected by the formation of the Leshan-Longnusi paleo-uplift and the differential evolution of structures, the final formation of the Dengying Formation gas fields mainly went through three evolutionary stages: the formation of paleo-oil pools, the cracking of paleo-oil pools, and the adjustment of oil-cracking gas pools (Figure 12).

Oil pool formation stage: The Ordovician-Silurian corresponds to the initial oil-generation stage, while the Permian-Middle Triassic corresponds to the secondary oil-generation stage. By the end of the Ordovician, the main source rocks of the Cambrian Qiongzhusi Formation experienced early shallow burial. Source rocks in the slopes and rift troughs of the paleo-uplift reached maturity, while those in structurally high areas remained less mature (Shi, 2017; Shuai et al., 2023). Rift-zone source rocks entered the oil generation window, and limited liquid hydrocarbon charging formed the first paleo-oil pools (Song et al., 2025) (Figure 11). Liquid hydrocarbon inclusions accounted for 90%, gas-liquid inclusions ~10%, with low gas-to-liquid ratios. Early Caledonian-Hercynian tectonic uplift terminated this initial oil generation until Permian deposition (Figure 8) (Shi et al., 2024). Since the Early Permian, lithospheric extension and elevated heat flow due to mantle plume activity triggered secondary oil generation.

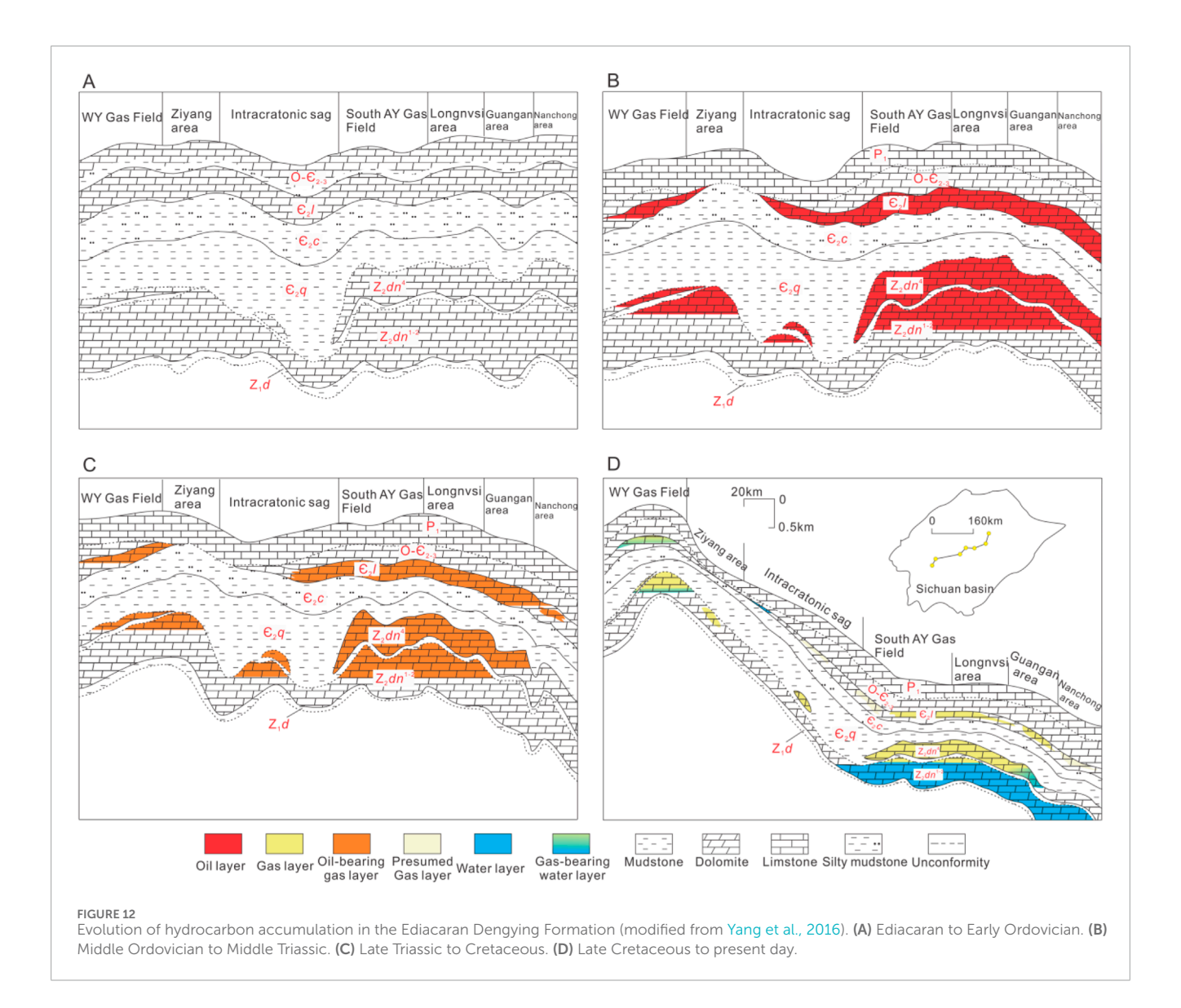


Source rocks from the paleo-uplift slopes to rift troughs and structurally high areas reached peak oil generation successively. Inclusions are dominated by gas-liquid phases, though gas-to-liquid ratios remain low. Homogenization temperatures overlap with the subsequent oil cracking stage, indicating continuous hydrocarbon charging in some areas. During this stage, gas charging occurred simultaneously (Fan et al., 2022; Deng et al., 2025). Liquid hydrocarbons migrated along unconformities and faults from the rift troughs and slopes to structurally high areas, forming large paleo-oil pools in the Central Sichuan paleo-uplift. In structurally high areas, such as the Ziyang area and Anyue area, large-scale paleo-oil pools are accumulated in the Dengying Formation, whereas slope areas including Weiyuan and Yongchuan may not have formed paleo-oil pools (Figure 12B).

Cracking stage of paleo-oil pools: Starting from the Late Triassic, the region entered a foreland basin evolution stage under the influence of the Indosinian orogeny, with further burial and heating of the strata. As the source rocks evolved into a high-to over-mature gas generation stage, previously formed paleo-oil pools or dispersed liquid hydrocarbons began to crack (Figure 8). By the Late Jurassic to Cretaceous, the Lower Cambrian source rocks had reached burial depths exceeding 5000 m and were in the peak gas generation period (Deng et al., 2023; Deng et al., 2025). Fluid inclusions are dominated by gas-phase hydrocarbons, primarily CH₄, with minor liquid hydrocarbon inclusions and bitumen, indicating ongoing oil cracking and continuous natural gas generation and charging. By the end of the Cretaceous, most paleo-oil had been cracked, and the oilcracking gas combined with gas generated directly from the source rocks began to accumulate again (Shuai et al., 2023; Wang et al., 2024). Paleo-oil pools formed in the structurally high parts of the early paleo-uplift gradually evolved into gas pools. As the high points of the traps began to migrate towards the Weiyuan area, the oilcracking gas in the western part of the paleo-uplift may be adjusted towards the WY Gas Field. Along with the formation of the Weiyuan structure, large-scale kerogen-cracking gas has been accumulated in the Dengying Formation reservoir in the Weiyuan area (Figure 12C).

Affected by the Himalayan Movement, large-scale tectonic movements occurred in the Sichuan Basin, resulting in significant adjustments to the Dengying Formation gas pool (Fan et al., 2022). The Eastern paleo-uplift in the Anyue area inherited subsidence, with a small degree of structural adjustment. Oilcracking gas were accumulated and preserved in situ, forming the current AY Gas Field. The Weiyuan area located in the western paleo-uplift experienced rapid uplift, and the formation of large dome structures led to the evolution of the high point of the Ziyang structure into the northern slope zone of the Weiyuan structure. The vast majority of oil-cracking gas in the Ziyang area has undergone readjustment and migration, forming the WY Gas Field, while only a small amount of oil-cracking gas remains in the Ziyang area (Figure 12D). In addition, traps of varying scales were formed from the paleo-uplift slope to the intracratonic sag, which may have captured late stage oil-cracking gas and formed new gas pools, such as the Dengying second Member gas pool in the Yongchuan area.

Based on the Ediacaran natural gas accumulation and evolution model, the Dengying Formation reservoirs experienced a complex "two-stage oil + three-stage gas" accumulation. The continuous oil-to-gas cracking during the gas pool adjustment phase serves as the key gas source, and its effective integration with tectonic events and other accumulation factors governs the efficiency and scale of late-stage gas accumulation. Considering the complex Himalayan tectonics, the formation and preservation of effective lithologic or compound traps before and after gas pool adjustment are identified as critical targets for future exploration.



5 Conclusions

- 1. The spatial relationship between deep dolomite reservoirs and source rocks results in variations in the sources of solid bitumen and natural gas across different regions. The quality of the Cambrian Maidiping source rock is superior to that of the Qiongzhusi source rock. The kerogen type of Maidiping source rock is Type I, with high organic matter maturity and in the over-matured stage. The natural gas of Dengying Formation comes from a mixture of oil-cracking gas and kerogen-cracking gas. The genesis of natural gas vary greatly in different areas (or wells).
- 2. The natural gas in Dengying second Member of AY Gas Field is mainly composed of oil-cracking gas, while natural gas in fourth Member are mainly composed of oil-cracking gas. Oil-cracking gas accounts for about 60% of the natural gas in the north AY Gas Field, while the Dengying Formation of WY Gas Field is mainly composed of kerogen-cracking gas. The
- natural gas in the Dengying Formation mainly comes from the Qiongzhusi source rock, but the contribution of Maidiping and Ediacaran source rocks from different wells or areas to natural gas accumulation varies. The proportion of gas supply from the Maidiping source rock in the Dengying fourth Member of AY Gas Field and Dengying second Member of the Ziyang area is significantly higher.
- 3. The Qiongzhusi source rock entered the oil-generation period from the Late Silurian to the end of the Late Cretaceous tectonic uplift. The Permian and Triassic correspond to main oil-generation periods. The gas-generation period lasted from the Late Permian to the end of the Early Cretaceous, with the Jurassic being the main gas-generation period. Influenced by the formation and structural evolution of the Central Sichuan paleo-uplift, the hydrocarbon accumulation process of the Dengying Formation in South Sichuan Basin has gone through three evolutionary stages: the formation of paleo-oil pools during Caledonian-Hercynian period, the oil cracking stage

during Indosinian-Yanshanian period, and the adjustment stage of gas pools in the Himalayan period.

Data availability statement

The original contributions presented in the study are included in the article/supplementary material, further inquiries can be directed to the corresponding author.

Author contributions

HJ: Conceptualization, Investigation, Methodology, Writing – original draft, Writing – review and editing.

Funding

The authors declare that financial support was received for the research and/or publication of this article. This study was funded by the National Natural Science Foundation of China (Grant No. 42202166), and National Natural Science Foundation of China (Grant No. 41972165).

References

Al-Shami, T. M., Jufar, S. R., Kumar, S., Abdulelah, H., Abdullahi, M. B., Al-Hajri, S., et al. (2023). A comprehensive review of interwell interference in shale reservoirs. *Earth-Science Rev.* 237 (2023), 104327. doi:10.1016/j.earscirev.2023.104327

Bodnar, R. J. (1993). Revised equation and table for determining the freezing point depression of H₂O-NaCl solutions. *Geochim. Cosmochim. Acta.* 57 (3), 683–684. doi:10.1016/0016-7037(93)90378-A

Cao, Q. Y. (1985). Identification of micro-components and types of kerogen under transmitted light. *Pet. Explor. Dev.* 5, 14–23. doi:10.3787/j.issn.1000-0976.1985.05.002

Chang, X. C., Ge, T. C., Shi, B. B., Liu, Z., Xu, Y., and Wang, Y. (2022). Application of biomarker recovery method for oil-source correlation in severe to extreme biodegradation in eastern chepaizi uplift, junggar basin (NW China). *Energy Rep.* 8, 11865–11884. doi:10.1016/j.egyr.2022.09.017

Chen, Z. H., Simoneit, B. R. T., Wang, T., Yang, Y. M., Ni, Z. Y., Chen, B., et al. (2017). Biomarker signatures of sinian bitumens in the moxi-gaoshiti bulge of sichuan basin, China: geological significance for paleo-oil reservoirs. *Precambr. Res.* 296, 1–19. doi:10.1016/j.precamres.2017.04.038

Chen, G. S., Shi, X. W., Liu, Y., Wu, W., Yang, Y. R., Zhu, Y. Q., et al. (2024). New insights into controlling factors for deep shale gas enrichment of wufeng-longmaxi formations in the southern sichuan basin, China. *Nat. Gas. Ind.* 44 (1), 58–71. doi:10.3787/j.issn.1000-0976.2024.01.006

Dai, J. X., Pei, X. G., and Qi, H. F. (1992). Natural gas geology of China. Beijing: Petroleum Industry Press, 1–260.

Deng, B., Wu, J., Li, W. Z., Lu, P. D., Tian, T. Z., Jiang, H., et al. (2023). U-Pb dating and trapped hydrocarbon inclusions in carbonate for petroleum accumulation: case study from the sinian dengying formation in the central sichuan basin. *Nat. Gas. Geo.* 34 (1), 1887–1898. doi:10.11764/j.issn.1672-1926.2023.07.007

Deng, B., Liu, S. G., Yao, G. S., Liao, Y., Zhang, B. J., Zhang, H., et al. (2024). Distribution pattern and main controlling factors of Paleozoic giant- and medium-sized gas fields of the sichuan super gas basin in southwest China. *Nat. Gas. Ind.* 44 (7), 54–76. doi:10.3787/j.issn.1000-0976.2024.07.005

Deng, B., Lu, P. D., Li, Z. Q., Wu, J., Li, W. Z., Sun, W., et al. (2025). The process of hydrocarbon accumulation in the sinian dengying formation, Penglai gas field, central Sichuan Basin, constrained by bitumen morphology, low-temperature thermochronology, and fluid geochemistry. J. Chengdu Univ. Technol. Sci. Technol. Ed. 52 (4), 603–619. doi:10.12474/cdlgzrkx.2024042602

Fan, J. J., Jiang, H., Lu, X. S., Liu, Q., Liu, S. B., Ma, X. S., et al. (2022). Pressure evolution and hydrocarbon accumulation process of Sinian dengying

Conflict of interest

Author HJ was employed by CNPC Chuanqing Drilling Engineering Co.

Generative AI statement

The authors declare that no Generative AI was used in the creation of this manuscript.

Any alternative text (alt text) provided alongside figures in this article has been generated by Frontiers with the support of artificial intelligence and reasonable efforts have been made to ensure accuracy, including review by the authors wherever possible. If you identify any issues, please contact us.

Publisher's note

All claims expressed in this article are solely those of the authors and do not necessarily represent those of their affiliated organizations, or those of the publisher, the editors and the reviewers. Any product that may be evaluated in this article, or claim that may be made by its manufacturer, is not guaranteed or endorsed by the publisher.

formation gas reservoirs in the penglai area, Sichuan Basin. *Nat. Gas. Ind.* 42, 32–43. doi:10.3787/j.issn.1000-0976.2022.12.004

Fang, X. Y., Deng, B., Geng, A. S., Liu, S. F., Wang, P. F., Liang, X., et al. (2024). Geochemical properties, mechanism of formation, and source of solid bitumen in the Ediacaran dengying Formation from the central to northern sichuan basin, China. *Mar. Pet. Geol.* 159, 106573. doi:10.1016/j.marpetgeo.2023.106573

Goldstein, R. H. (2001). Fluid inclusions in sedimentary and diagenetic systems. *Lithos* 55 (1), 159–193. doi:10.1016/S0024-4937(00)00044-X

Gu, Y. F., Zhou, L., Jiang, Y. Q., Jiang, C., Luo, M. S., and Zhu, X. (2019). A model of hydrothermal dolomite reservoir facies in Precambrian dolomite, central sichuan basin, SW China and its geochemical characteristics. *Acta Geol. Sin. Engl. Ed.* 93, 130–145. doi:10.1111/1755-6724.13770

Gu, Y. F., Wang, Z. L., Yang, C. C., Luo, M. S., Jiang, Y. Q., Luo, X. R., et al. (2023). Effects of diagenesis on quality of dengying formation deep dolomite reservoir, central sichuan basin, China: insights from petrology, geochemistry and in situ U-Pb dating. Front. Earth Sci. 10, 1041164. doi:10.3389/feart.2022.

Guo, X. S., Huang, R. C., Zhang, D. W., Li, S. J., Shen, B. J., and Liu, T. J. (2024). Hydrocarbon accumulation and orderly distribution of whole petroleum system in marine carbonate rocks of sichuan basin, SW China. *Pet. Explor. Dev.* 51 (4), 852–869. doi:10.1016/s1876-3804(24)60511-2

Hagstrom, C. A., Hubbard, S. M., Horner, S. C., Martin, H. K., and Peng, Y. (2024). Comparison of the morphology, facies, and reservoir quality of valley fills in the southern athabasca oil sands region, Alberta, Canada. *AAPG Bull.* 107 (4), 553–591. doi:10.1306/10242219118

Hattori, K. E., and Radjef, E. M. (2024). Lithologic controls on reservoir quality and production trends in the pettet formation, rusk county, east Texas. *AAPG Bull.* 108 (3), 401–419. doi:10.1306/11022322150

Hou, D. J., and Liu, Z. H. (2011). Petroleum geochemistry (book). Beijing: Petroleum Industry Press, 1–98.

Hou, L. L., Yang, F., Yang, C., and Wang, J. H. (2021). Characteristics and formation of sinian (ediacaran) carbonate karstic reservoirs in dengying formation in sichuan basin, China. *Pet. Res.* 6, 144–157. doi:10.1016/j.ptlrs.2020.11.003

Larue, D., Allen, J., Audinet, C., Miller, K., and Thompson, J. (2024). Complex multiscale reservoir heterogeneity in a tidal depositional environment, temblor formation, west coalinga field, California. *AAPG Bull.* 108 (1), 107–157. doi:10.1306/01172320199

- Li, S. J., Gao, P., Huang, B., and Wang, H. J. (2018). Sedimentary constraints on the tectonic evolution of mianyang–changning trough in the sichuan basin. *Oil Gas. Geol.* 39 (5), 889–898. doi:10.11743/ogg20180504
- Li, R., Wang, Y. X., Wang, Z. C., Xie, W. R., Li, W. Z., Gu, M. F., et al. (2023). Geological characteristics of the southern segment of the late sinian–early Cambrian deyang–anyue rift trough in sichuan basin, SW China. *Pet. Explor. Dev.* 50 (2), 321–333. doi:10.1016/s1876-3804(23)60390-8
- Li, Q., Zhu, G. Y., and Zhang, Z. Y. (2024). Genesis and control factors of ultra-deep dolomite reservoirs: case study of the sinian Dengying Formation and Cambrian Longwangmiao Formation, Sichuan Basin, China. Sci. China Earth Sci. 54 (7), 2389–2418. doi:10.1360/SSTe-2023-0164
- Liu, Y. (2022). Geochemical characteristics of Lower Cambrian source rocks in middle and upper yangtze region. Beijing: China University of Petroleum.
- Liu, W., Qiu, N. S., Xu, Q. C., and Liu, Y. F. (2018). Precambrian temperature and pressure system of gaoshiti-moxi block in the central paleo-uplift of sichuan basin, southwest China. *Precambr. Res.* 313, 91–108. doi:10.1016/j.precamres.2018. 05 028
- Luemba, M., Chen, Z. H., and Ntibahanana, J. (2021). Molecular markers of neoproterozoic-lower Paleozoic petroleum systems and their geological significance: a case study of the cratonic basins in Western China. *J. Petroleum Sci. Eng.* 204 (2021), 108707. doi:10.1016/j.petrol.2021.108707
- Luo, T., Guo, X. W., He, Z. L., Yun, N. H., Tao, Z., and Wang, F. R. (2024). Determination of multistage oil charge processes in the Ediacaran dengying gas reservoirs of the Southwestern sichuan basin, SW China. *Mar. Pet. Geol.* 164, 106853. doi:10.1016/j.marpetgeo.2024.106853
- Ma, X. H., Yang, Y., Wen, L., and Luo, B. (2019). Distribution and exploration direction of medium- and large-sized marine carbonate gas fields in sichuan basin, SW China. *Pet. Explor. Dev.* 46 (1), 1–15. doi:10.1016/s1876-3804(19)30001-1
- Pickel, W., Kus, J., Flores, D., Kalaitzidis, S., Christanis, K., Cardott, B. J., et al. (2017). Classification of liptinite-ICCP system 1994. *Int. J. Coal Geol.* 169, 40–61. doi:10.1016/j.coal.2016.11.004
- Prather, B. E., Goldstein, R. H., Kopaska-Merkel, D. C., Heydari, E., Gill, K., and Minzoni, M. (2023). Dolomitization of reservoir rocks in the smackover formation, southeastern Gulf Coast, U.S.A. *Earth-Science Rev.* 244 (2023), 104512. doi:10.1016/j.earscirev.2023.104512
- Shi, Y. Z., Wang, Z. C., Xu, Q. C., Hu, S. B., Huang, S. P., Jiang, H., et al. (2024). Thermal history restoration of superimposed basins and applications: case study of sinian–Cambrian strata in central Sichuan Basin. *Nat. Gas. Ind.* 44 (8), 29–43. doi:10.3787/j.issn.1000-0976.2024.08.003
- Shuai, Y. H., Li, J., Tian, X. W., Chen, Z. X., Zhang, B., and Wei, C. Y. (2023). Accumulation mechanisms of sinian to Triassic gas reservoirs in the central and Western sichuan basin and their significance for oil and gas prospecting. *Acta Geol. Sin.* 97 (5), 1526–1543. doi:10.19762/j.cnki.dizhixuebao.2023227
- Song, Z. Z., Jin, S. G., Luo, B., Luo, Q. Y., Tian, X. W., Yang, D. L., et al. (2025). Geochemical characteristics and genesis of natural gas in the sinian dengying formation on both sides of deyang–Anyue rift trough, Sichuan Basin, China. *Pet. Explor. Dev.* 52 (2), 374–384. doi:10.11698/PED.20240289
- Su, A., Chen, H. H., Feng, Y. X., Zhao, J. X., Wang, Z. C., Hu, M. Y., et al. (2022). *In situ* U-Pb dating and geochemical characterization of multi-stage dolomite cementation in the Ediacaran dengying Formation, Central sichuan basin, China: constraints on diagenetic, hydrothermal and paleo-oil filling events. *Precambr. Res.* 368, 106481. doi:10.1016/j.precamres.2021.106481
- Sun, W., Liu, S. G., Song, J. M., Deng, B., Wang, G., Wu, J., et al. (2017). Formation process and characteristics of ancient and deep carbonate reservoirs in superimposed basins: case study of sinian (ediacaran) dengying formation in Sichuan Basin, China. *J. Chengdu Univ. Technol. Sci. Technol. Ed.* 44 (3), 257–285. doi:10.3969/j.issn.1671-9727.2017.03.01
- Sun, Y. T., Tian, X. W., Ma, K., Peng, H. L., Dai, H. M., Wang, H., et al. (2019). Carbon and hydrogen isotope characteristics and source of natural gas in shuangyushi gas reservoir, northwestern Sichuan Basin. *Nat. Gas. Geosci.* 30 (10), 1477–1486. doi:10.11764/j.issn.1672-1926.2019.05.001
- Tian, F. L., Wu, F. R., He, D. F., Zhao, X. H., Liu, H., Zhang, Q. Y., et al. (2023). Structural attributes, evolution and petroleum geological significances of the Tongnan negative structure in the central Sichuan basin, SW China. *Pet. Explor. Dev.* 50 (5), 1120–1136. doi:10.1016/S1876-3804(23)60453-7
- Wang, H. J., Jiang, Y. Q., Yang, C. C., Zhang, B. S., Gu, Y. F., Luo, X. R., et al. (2023). Hydrothermal silicification in Ediacaran dengying formation fourth member deep dolomite reservoir, central Sichuan Basin, China: implications for reservoir quality. *Geol. J.* 58, 4257–4270. doi:10.1002/gj.4757
- Wang, Z. C., Zhao, Z. Y., Huang, F. X., Shi, Y. Z., Xu, Y., and Zhang, S. (2024). Conditions and exploration potential of deep oil and gas accumulation in oil-bearing basins of central and Western China. World pet. *Ind* 31 (1), 33–48. doi:10.20114/j.issn.1006-0030.20231202001
- Wang, Z. L., Jiang, C., Yang, C. C., Jiang, Y. Q., and Gu, Y. F. (2025). Hydrothermal activity and its influence on hydrocarbon accumulation in deep dolomite reservoirs

- of the Ediacaran dengying formation, sichuan basin. $\it Energy~Geosci.~6$ (2025), 100370. doi:10.1016/j.engeos.2024.100370
- Wei, G. Q., Xie, Z. Y., Song, J. R., Yang, W., Wang, Z. H., Li, J., et al. (2015). Features and origin of natural gas in the sinian–cambrian of central sichuan paleo-uplift, sichuan basin, SW China. *Pet. Explor. Dev.* 42 (6), 768–777. doi:10.1016/s1876-3804(15)30073-2
- Wei, G. Q., Yang, W., Xie, W. R., Su, N., Xie, Z. Y., Zeng, F. Y., et al. (2022). Formation mechanisms, potentials and exploration practices of large lithologic gas reservoirs in and around an intracratonic rift: taking the Sinian–Cambrian of sichuan basin as an example. *Pet. Explor. Dev.* 49 (3), 530–545. doi:10.1016/s1876-3804(22)60044-2
- Whiticar, M. J. (1993). Stable isotopes and global budgets. Berlin: Springer Berlin Heidelberg.
- Whiticar, M. J. (1999). Carbon and hydrogen isotope systematics of bacterial formation and oxidation of methane. *Chem. Geol.* 161, 291–314. doi:10.1016/S0009-2541(99)00092-3
- Worden, R. H., Griffiths, J., Wooldridge, L. J., Utley, J. E. P., Lawan, A. Y., Muhammed, D. D., et al. (2020). Chlorite in sandstones. *Earth-Science Rev.* 204 (2020), 103105. doi:10.1016/j.earscirev.2020.103105
- Xie, N., Song, J. Q., Bai, D., and Zou, X. J. (2023). Characteristics of fluid inclusions and accumulation stages of sinian dengying formation in penglai area, central sichuan. *Unconv. Oil Gas.* 10 (3), 55–63. doi:10.19901/j.fcgyq.2023.03.08
- Xu, F. H., Xu, G. S., Liang, J. Y., Yuan, H. F., Liu, J. J., and Xu, F. G. (2016). Multistage fluid charging and critical period of hydrocarbon accumulation of the sinian dengying formation in central sichuan basin. *Acta Geol. Sin. Engl. Ed.* 90, 1549–1550. doi:10.1111/1755-6724.12791
- Xu, C., Shan, X., He, W., Zhang, K., Rexiti, Y., Su, S., et al. (2021). The influence of paleoclimate and a marine transgression event on organic matter accumulation in lacustrine Black shales from the Late cretaceous, southern songliao basin, northeast China. *Int. J. Coal Geol.* 246, 103842. doi:10.1016/j.coal.2021.103842
- Xu, C., Peng, G. R., Liu, P., He, Y., Jia, P. M., Shan, X. L., et al. (2025). The evolution of organic matter sources and sedimentary environments in lakes during the Eocene climatic optimum. *Mar. Petroleum Geol.* 181 (2025), 107496. doi:10.1016/j.marpetgeo.2025.107496
- Yang, Y. M., Wen, L., Luo, B., Wang, W. Z., and Shan, S. J. (2016). Hydrocarbon accumulation of Sinian natural gas reservoirs, leshan-longnusi paleohigh, sichuan basin, SW China. *Pet. Explor. Dev.* 43 (2), 197–207. doi:10.1016/s1876-3804(16)30023-4
- Yang, W., Wei, G. Q., Xie, W. R., Jin, H., Zeng, F. Y., Su, N., et al. (2020). Hydrocarbon accumulation and exploration prospect of mound-shoal complexes on the platform margin of the fourth member of sinian Dengying Formation in the east of Mianzhu–changning intracratonic rift, sichuan basin, SW China. *Pet. Explor. Dev.* 47 (6), 1262–1274. doi:10.1016/s1876-3804(20)60134-9
- Yang, M., Pan, Y., Feng, H., Yan, Q., Lu, Y., Wang, W., et al. (2025). Fractal characteristics of pore structure of longmaxi shales with different burial depths in Southern Sichuan and its geological significance. *Fractal Fract.* 9, 2. doi:10.3390/fractalfract9010002
- Ye, Y., Jiang, Z., Liu, X., Wang, Z., and Gu, Y. (2024). Logging identification method for reservoir facies in fractured-vuggy dolomite reservoirs based on AI: a case study of Ediacaran dengying formation, Sichuan Basin, China. *Appl. Sci.* 14, 7504. doi:10.3390/app14177504
- Yong, R., Shi, X. W., Luo, C., Zhong, K. S., Wu, W., Zheng, M. J., et al. (2024). Aulacogen-uplift enrichment pattern and exploration prospect of Cambrian qiongzhusi formation shale gas in sichuan Basin, SW China. *Petroleum Explor. Dev.* 51 (6), 1402–1420. doi:10.1016/s1876-3804(25)60549-0
- Yong, R., Wu, J. F., Wu, W., Yang, Y. R., Xu, L., Luo, C., et al. (2024). Discovery and significance of shale gas in Cambrian qiongzhusi formation, southern Sichuan Basin, China. *Acta Pet. Sin.* 45 (9), 1309–1323. doi:10.7623/syxb202409001
- Zeng, F. Y., Yang, W., Wei, G. Q., Yi, H. Y., Zeng, Y. X., Zhou, G., et al. (2023). Structural features and exploration targets of platform margins in sinian dengying formation in deyang-anyue rift, Sichuan Basin, SW China. *Pet. Explor. Dev.* 50 (2), 306–320. doi:10.1016/s1876-3804(23)60389-1
- Zhang, S. C., He, K., Hu, G. Y., Mi, J. K., Ma, Q. S., Liu, K. Y., et al. (2018). Unique chemical and isotopic characteristics and origins of natural gases in the Paleozoic marine formations in the sichuan basin, SW China: isotope fractionation of deep and high mature carbonate reservoir gases. *Mar. Pet. Geol.* 89, 68–82. doi:10.1016/j.marpetgeo.2017.02.010
- Zhao, W. Z., Xie, Z. Y., Wang, X. M., Shen, A. J., Wei, G. Q., Wang, Z. C., et al. (2021). Sinian gas sources and effectiveness of primary gas-bearing system in sichuan basin, SW China. *Pet. Explor. Dev.* 48 (6), 1260–1270. doi:10.1016/s1876-3804(21)60285-9
- Zheng, D. Y., Pang, X. Q., Luo, B., Chen, D. X., Pang, B., Li, H. Y., et al. (2021). Geochemical characteristics, genetic types, and source of natural gas in the sinian dengying formation, Sichuan Basin, China. *J. Pet. Sci. Eng.* 199, 108341. doi:10.1016/j.petrol.2020.108341
- Zhu, H. J., Ju, Y. W., Lu, Y. J., Yang, M. P., Feng, H. Y., Qiao, P., et al. (2025). Natural evidence of organic nanostructure transformation of shale during bedding-parallel slip. *GSA Bull.* 137 (5/6), 2719–2746. doi:10.1130/B37712.1